EFFECT OF DUCT SPACING ON BREAKOUT OF POST-TENSIONING TENDONS IN HORIZONTALLY CURVED CONCRETE BOX GIRDERS

APPROVED:

Supervisor:____________________________
Dr. John E. Breen

____
Dr. Michael E. Kreger

To my mother, father and sister

EFFECT OF DUCT SPACING ON BREAKOUT OF POST-TENSIONING TENDONS IN HORIZONTALLY CURVED CONCRETE BOX GIRDERS

by

DEEPAK AHUJA, B.E.(Mech.), B.E.(Civil)

REPORT

Presented to the Faculty of the Graduate School of
The University of Texas at Austin
in Partial Fulfillment
of the Requirements
for the Degree of
Master of Science in Engineering

THE UNIVERSITY OF TEXAS AT AUSTIN
August, 1991

ACKNOWLEDGEMENT

This research program was conducted under the guidance of Dr. John E. Breen at the Phil M. Ferguson Structural Engineering Laboratory at the Balcones Research Center of the University of Texas at Austin. I am grateful to Dr. Breen whose guidance, moral support and wise counsel contributed to my education as an engineer and also as a person. I am thankful to Dr. Michael E. Kreger for his invaluable comments and suggestions.

I would like to thank Blake Stasney, Pat Ball, Alec Tahmassebi Wayne Little and Wayne Fontenot for their technical assistance and practical knowledge. Without their dedication, hard work and technical insight this research would have been difficult if not impossible.

I express my gratitude to my good friend Dean Van Landyut who helped me to adjust to the American way of life in and outside the lab. I thank him for teaching me the right technique to sweep the floor and hit a nail with a hammer. I thank Santiago Lopez for all his help in instrumentation of the specimen and his keen sense of humor during the course of the project. Special thanks to Carin Roberts, Karin Ryals, Jose Pincheira, Abdelhakim Boudi and Swarnalatha Vegesna who taught me the intricacies of computer software I used for this research.

It was an interesting experience to work at the Ferguson laboratory as it gave me an opportunity to meet and work with a group of diversified, talented and fine people. It provided an opportunity to learn about different cultures and make friends from different countries. Some friends I would like to mention are Gregor Wollmann, Asit Baxi, Vekatesh Iyer, Bruce Russel, Les Zumbrunnen, Raj Valluvan, Reed Freeman, Todd Helwig, Gilberto Leiva, Chris Tansil, Syed Wahidi, Imran Jalil and Leonard Joanes.

My gratitude to Dr. Richard E. Klingner who influenced me to join the graduate Structural Engineering program at the University of Texas at Austin and introduced me to the Ferguson laboratory.

Special thanks to my old friend and room mate in Austin, Shubneesh Batra for being patient with me and providing motivation and support during times of frustration.

I express my gratitude to my teachers at the University of Texas at Austin, the Birla Institute of Technology, and the Methodist High School without whom I would not achieved what I have. Special thanks to my tutor and mentor, Mr. Gupta who motivated me during a difficult period in my life from 1981-1983.

My deepest thanks to my parents Kavita and Srichandlal Ahuja and sister Jyoti. It is to them I owe my achievement. Their unrelenting encouragement, support and praise has given me the confidence I needed to pursue my goals. They will always have my respect and love.

Deepak Ahuja
May 31, 1991
Austin, Texas.

Table of Contents

Chapter Page No.

Table of Contents(Continued)

Chapter Page No.

List of Tables

List of Figures

List of Figures(Continued)

Figure Page No.

Chapter 1
INTRODUCTION

1.1 Background

Curved highway/railroad bridges are provided between two straight sections for a smooth and comfortable change in direction. Curved elevated roadways/railroads are used for constructing approach ramps to a straight/curved bridge over a river. The bridge location and geometry is often determined by the stream depth and the foundation characteristics of the river bed. To take care of the increased volume of traffic in the urban areas it is a common practice nowadays to provide elevated roadways/railroads. These highways and railroads are often curved to go around high rise buildings and other natural/man-made obstructions. Topography of the land and the requirement to have an intersection in a narrow piece of land also dictate the provision of an elevated curved roadway. Post-tensioned segmental concrete box girders are commonly used for the construction of medium to moderately long span highway/railroad bridges and elevated roadways. In these bridges the individual segments(box girders) are assembled together longitudinally or transversely by post-tensioning. The box girders can be either cast-in-place, precast, or a combination of precast and cast-in-place. Since post-tensioned segmental construction is a safe, fast and an economical method, it has been widely accepted for constructing elevated roads and bridges.

Eugene Freyssinet, often referred to as the father of prestressed concrete was the first designer to use precast segmental construction for prestressed concrete bridges. He designed such a bridge at Luzancy in France over the river Marne in 1945. Later, five similar bridges were built over the river Marne. Shortly after its success, segmental bridge construction became accepted in West Germany and then in other parts of Western Europe. More than 300 structures using the segmental construction method were erected between 1950 and 1965 in Europe alone. The interesting concept then spread to other parts of the world. The first segmental bridge in the United States was a single span county bridge located near Sheldon, New York. It was designed by Freyssinet Company in 1952. This bridge had longitudinal girder segments. The concept of transverse segments was still under development in Europe.

Box girders have evolved as the most efficient and least expensive of the segmental techniques. Box girder decks constructed using the balanced cantilever method were initially erected by being made integral with the piers while a special expansion joint was provided at the center of each span to allow for volume changes and to control differential deflections between individual cantilever arms. Because of objectionable creep deflections in these non-continuous systems, most structures now are constructed continuous over several spans with bearings provided between the girder and piers for expansion.

In cast-in-place segmental construction, the segments are cast one after another. Special equipment such as travellers for cantilever construction or mobile formwork moving along a supporting gantry for span by span construction are required for cast-in-place construction. Each segment is reinforced with conventional steel and sometimes by transverse and/or longitudinal prestressing while the assembly of segments in the longitudinal direction is done by post-tensioning. Joints are made to be watertight and safe enough to resist bending and shear stresses.

In precast segmental construction, segments are mass produced in a nearby plant or a factory under well controlled match casting conditions. After casting, the segments are transferred to the bridge site for final positioning and assembly. The match casting technique is almost universally used nowadays, in which the segments are cast against each other in the same order as they are required to be assembled. Before the match casting technique was developed, joints used to be either filled with wet concrete or packed with dry mortar. The major advantage of precast segments is that they can be cast well before the time of assembly and can attain substantial strength before post-tensioning. This reduces the deflections during construction and minimizes the effects of shrinkage and creep in the assembled bridge. Such precast match cast segmental box girders are being used in the San Antonio Y.

Both cast-in-place and precast box girders are widely used. The choice of the type of box girder depends very much on local conditions. The local conditions include size of the project, time of construction, environmental concerns, aesthetics, availability of equipment and capability of the contractor.

1.2 Literature Review

Problems in post-tensioned box girders have been known to occur whenever the beam is curved in its longitudinal dimension.These problems range from minor damage to complete rupture of the webs. The problems due to horizontal curvature of the post-tensioned segmental bridges were generally ignored in the past since there had not been any major distress. However, this changed with the catastrophic failures of the Kapioloni ramp in Hawaii(References 3 & 4) and the Las Lomas bridge in California(References 3 & 5). High lateral forces(in the radial direction) are induced in the web due to horizontal curvature of the longitudinal tendons(Figure 1.1). These forces are a major reason for the breakout of tendons in the curved region of the girder. Both the Kapioloni and the Las Lomas failure were explosive and loud. It was fortunate that no one was injured in either of the failures.

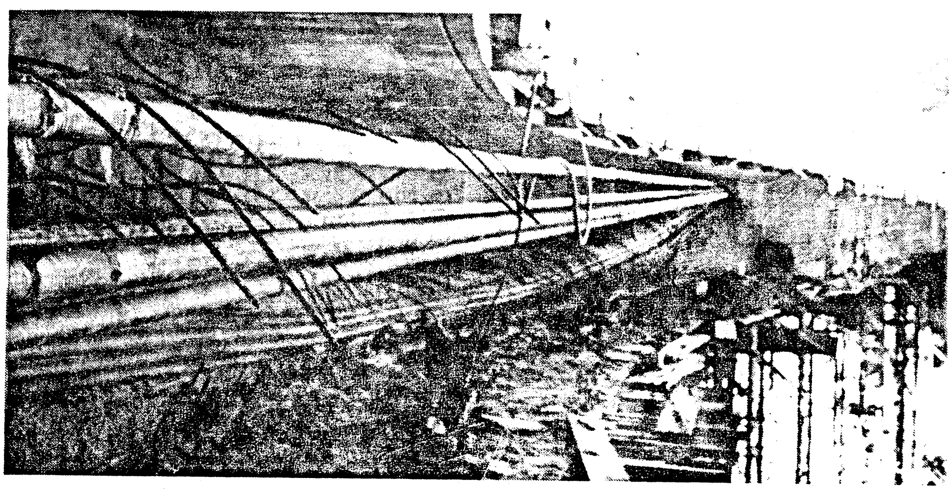

Figure 1.1 Failure of the Las Lomas Bridge(Reference 3)

This type of failure is dangerous and poses a threat to construction workers and surrounding traffic. This failure adds to the cost of the structure since the bridge will require retrofitting or replacement. The delay caused by failure, other legal and investigative costs, and the cost of replacement could add millions of dollars to the initial cost. In both these disastrous failures, there existed a combination of: 1) sharp horizontal curvature in the longitudinal direction of the tendon, 2) thin concrete cover over the tendons, 3) bundling of tendons, 4) large post-tensioning forces and 5) inadequate reinforcement in the webs. Failure may have been avoided with improvement in any one or more of these variables. It is impractical to change the alignment(radius of curvature) of the structure since it depends on the terrain and topography of the region. It is a common practice by designers in Texas to space the ducts at least one duct diameter clear to decrease the lateral force concentration. This kind of duct positioning restricts the eccentricity of the tendons. This leads to a less than optimum design for carrying vertical/gravity loads as post-tensioning is most effective when eccentricity of the tendons is a maximum.

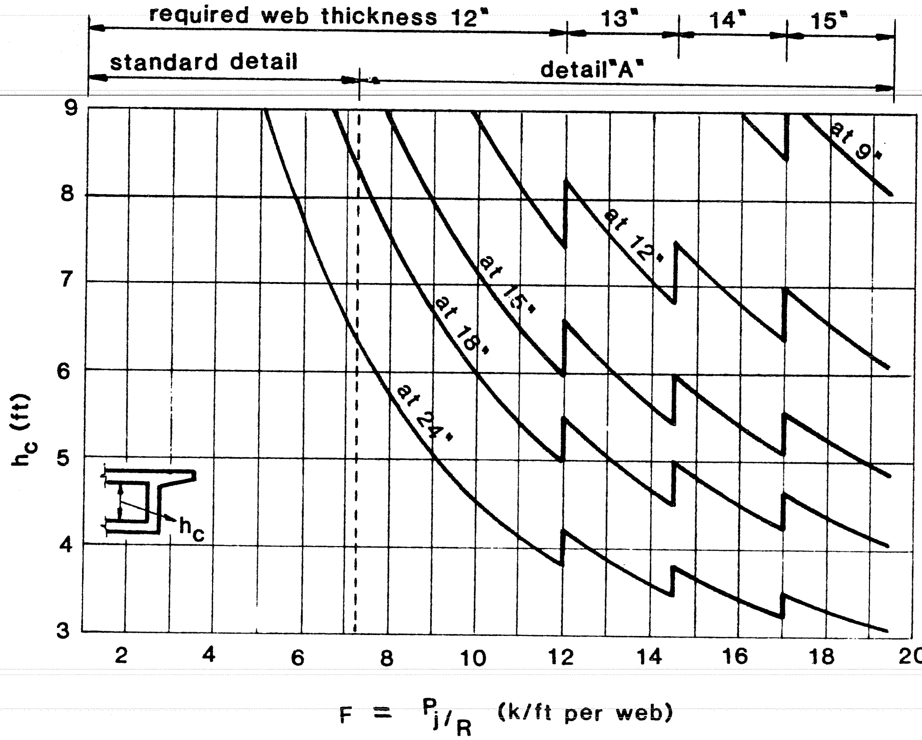

Figure 1.2 Chart For #5 Stirrups;(Reference 3)

The California Department of Transportation(CALTRANS) has prepared and implemented a detailing guideline for curved tendons in which provisions vary with height of web, the ratio of jacking force and radius of curvature. These recommendations are based on theoretical studies and have not been tested in the laboratory. CALTRANS has prepared charts for various reinforcing bars as shown in Figure 1.2. These charts suggest that detail "A" should be provided for high jacking force and sharp curves. The suggested detail "A" recommends greater cover on the inside of the curve as shown in Figure 1.3

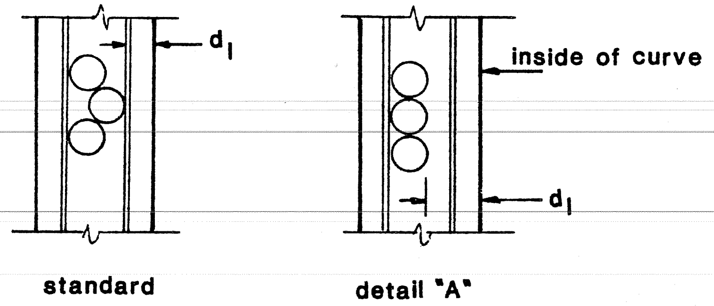

Figure 1.3 Tendon Placement Details;(Reference 3)

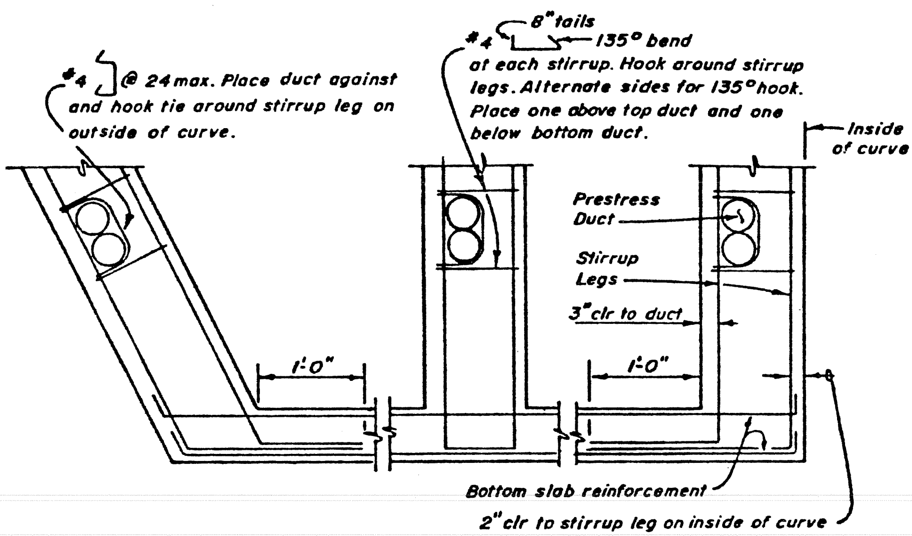

Figure 1.4 Tendon Placement Detail "A"; (Reference 3)

and specifies the provision of one hooked tie around the stirrup above and below the tendons as shown in Figure 1.4. It also recommends a tie around the ducts on the inside of the curve. The charts of Figure 1.2 also suggest closer stirrup spacing with an increase in the height of the web.

1.3 Objective and Scope

The broad objectives of this research are:

1) To start a pilot program to investigate the cause of problems in horizontally curved box girders during post-tensioning.

2) To develop testing facilities and procedures for testing horizontally curved box girders during post-tensioning.

3) To evaluate the effect of duct spacing on the behavior of horizontally curved box girders during post-tensioning.

4) To investigate the mechanism of radial load resistance of the horizontally curved box girders during post-tensioning.

The immediate objectives of the research program are outlined in Chapter 2, Section 2.1. The scope of the experimental program is to design and construct a test model of a single cell box section girder simulating a contemporary segmental bridge design. It also includes designing and building the load setup.

1.4 Summary of Following Chapters

This report is organized in six chapters. Chapter 2 describes the test design and the specimen design. The immediate objectives of the test program are outlined in Section 2.1. Section 2.2 describes the specimen in detail including the duct layout, choice of material and reinforcing details of the members. The basis of the model and the reasons for selecting the scale factor are also discussed. Section 2.3 describes the test setup which includes the loading concept and the safety features incorporated.

Chapter 3 describes the construction of the specimen.

Chapter 4 records the instrumentation used and the test procedure. Section 4.1 lists the objectives of the instrumentation. Section 4.2 describes the devices used in the test program and the location of the devices on the specimen. Section 4.3 outlines the test procedure in detail.

Chapter 5 presents the results of two tests while the final Chapter contains conclusions and recommendations.

Chapter 2
TEST AND SPECIMEN DESIGN

2.1 Test Objectives

In order to study the behavior of horizontally curved box girders during post-tensioning, this study had the following immediate test objectives:

1) Investigate the behavior of the web in the curved portion of the specimen. How does the web perform? Does the web fail in a ductile manner or is the failure sudden and brittle?

2) Study how the web resists the breakout forces. Does the web behave as a beam or does the concrete cover over the tendons act as a local slab to resist the breakout forces?

3) Study the effect of spacing of the ducts. Is there a difference in performance of web with duct spacing of 1.75" clear from that of a web with no clear spacing in the vertical direction in the curved portion of the beam?

4) Determine the duct detail which gives the higher web capacity to the web. Does the web with bundled ducts or the web with one duct clear spacing in the vertical direction resist larger breakout forces?

5) Evaluate the design of the model with respect to details and overall performance. What is the specimen behavior in the anchorage zone ? Is the length of the transition zone sufficient and do splices and laps develop the reinforcement ?

6) Recommend an alternate design approach. Can a suitable model be established from the test data and a safer design approach than the existing one be suggested?

7) Evaluate the loading procedure and instrumentation details. Is the test procedure adopted satisfactory and the information obtained useful and sufficient ? Is there a need to modify and improve upon the loading procedure and instrumentation?

2.2 Specimen Description

2.2.1 Basis for the Model: The specimen constructed is a one third scale model in cross-section of the failed Las Lomas bridge. However, the radius of curvature of the model was altered from the scaled prototype in order to produce higher radial loads and to facilitate construction. The box section chosen(Figure 2.1) is a typical single cell box section used for segmental bridges. Though the Las Lomas bridge had a two cell box section, it was considered unnecessary to have a two cell box section. The two cell box section would have led to complications in construction and increased cost. The straight portion of the specimen or the transition zone(Figure 2.2) was provided to withstand the anchorage forces due to post-tensioning and to develop uniform stress fields in the curved portion. The specimen was constructed and tested in an inverted position for simplicity and to ease construction and testing. Since the specimen was not loaded in the vertical direction, this should not affect the test results.

2.2.2 Scale Factor: A linear one third scale factor was adopted for the specimen. It was important to choose a convenient scale factor. If the scale factor is too big then the specimen cost would be exorbitant and the size of the testing equipment required would be unrealistically large. Safety of the laboratory personnel was another factor in keeping the scale factor small. Too small a scale factor would lead to tiny specimens which may not reveal the true effect of the local behavior of the specimen. Such small specimens would be difficult to construct as the placement of reinforcing bars and ducts would be critical.

2.2.3 Dimension of the Model: The specimen end view and plan are shown in Figure 2.1 & 2.2. The outer web has a radius of 22' while the inner web has a radius of curvature of 18'. The width of the bottom slab in plan is 7'. The distance between the center lines of the web is 4'. Other dimensions are one third scale of the Las Lomas Bridge. The dimension of the overhang was chosen to represent a common segmental box girder.

2.2.4 Layout of Ducts and Strands: The duct layout is illustrated in Figure.2.3. The web(R=18') which has ducts spaced at a distance of one duct diameter(1.75"OD) in the curved region of the beam is named DC(See Figure 2.4). The web(R=22') with ducts banded together in the curved region is

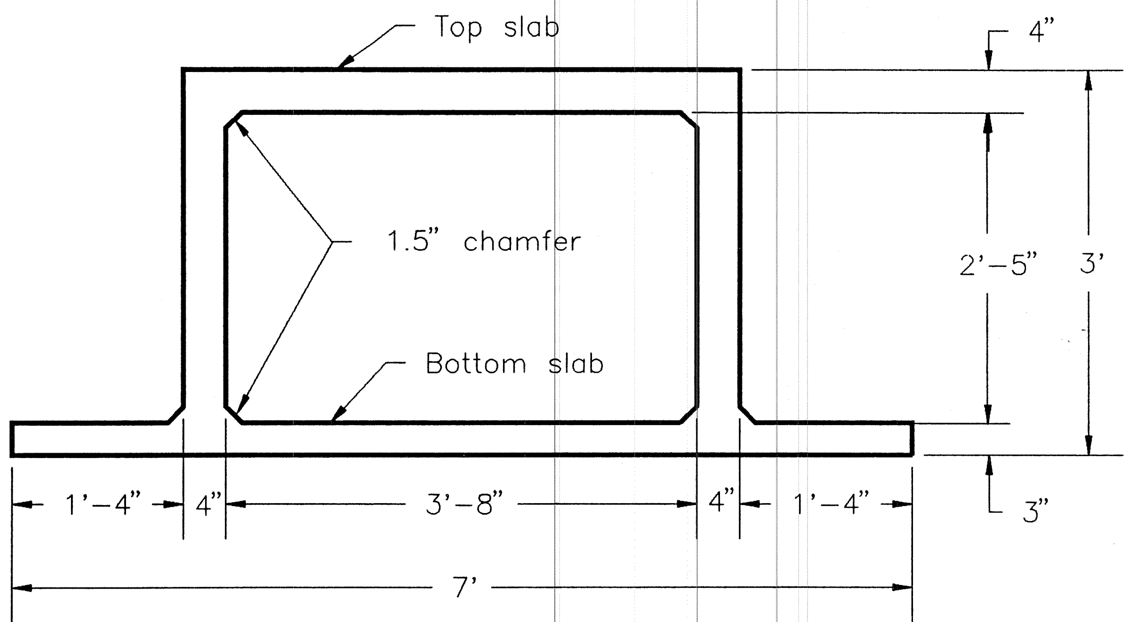

Figure 2.1 End View of Specimen

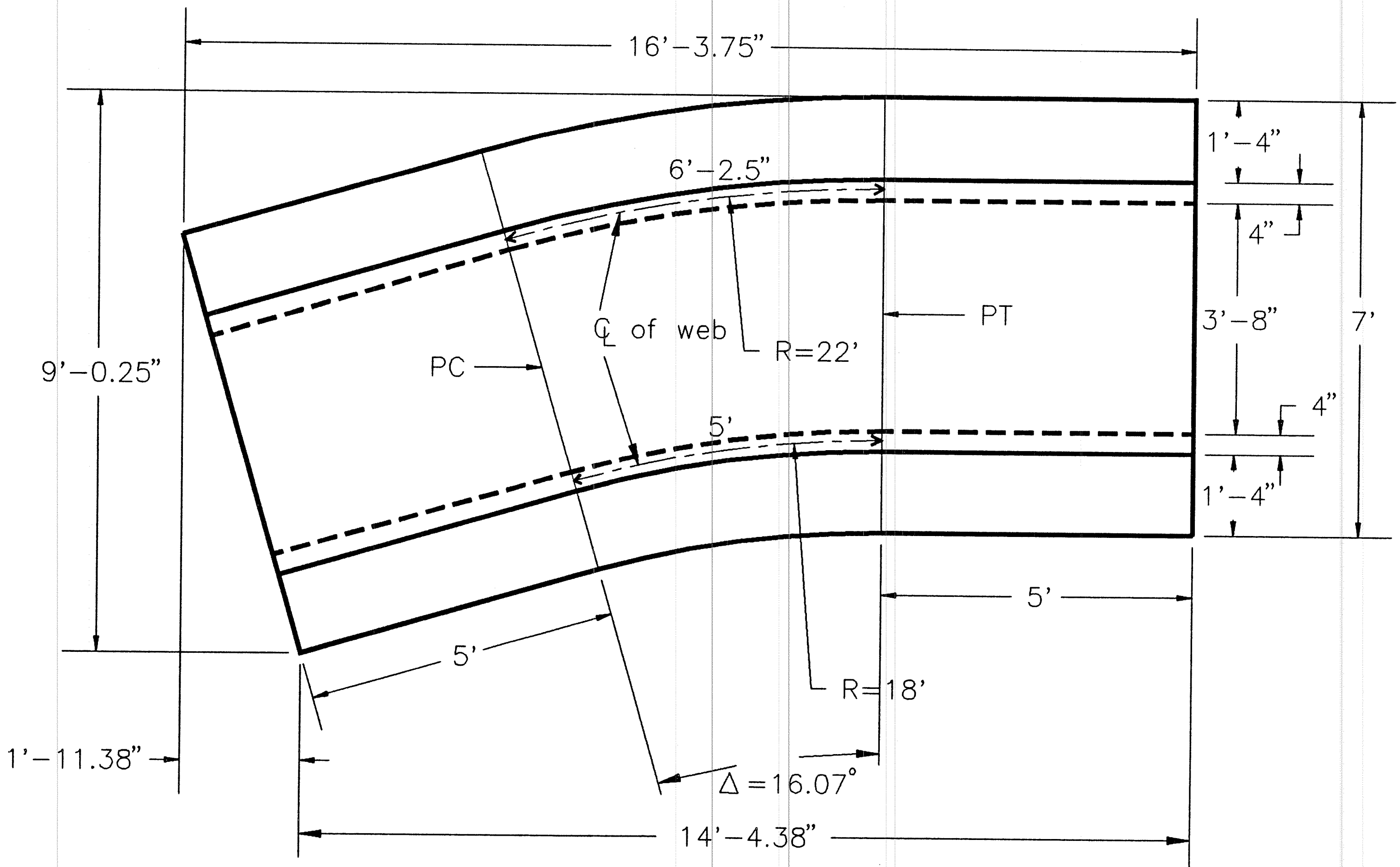

Figure 2.2 Plan View of Specimen

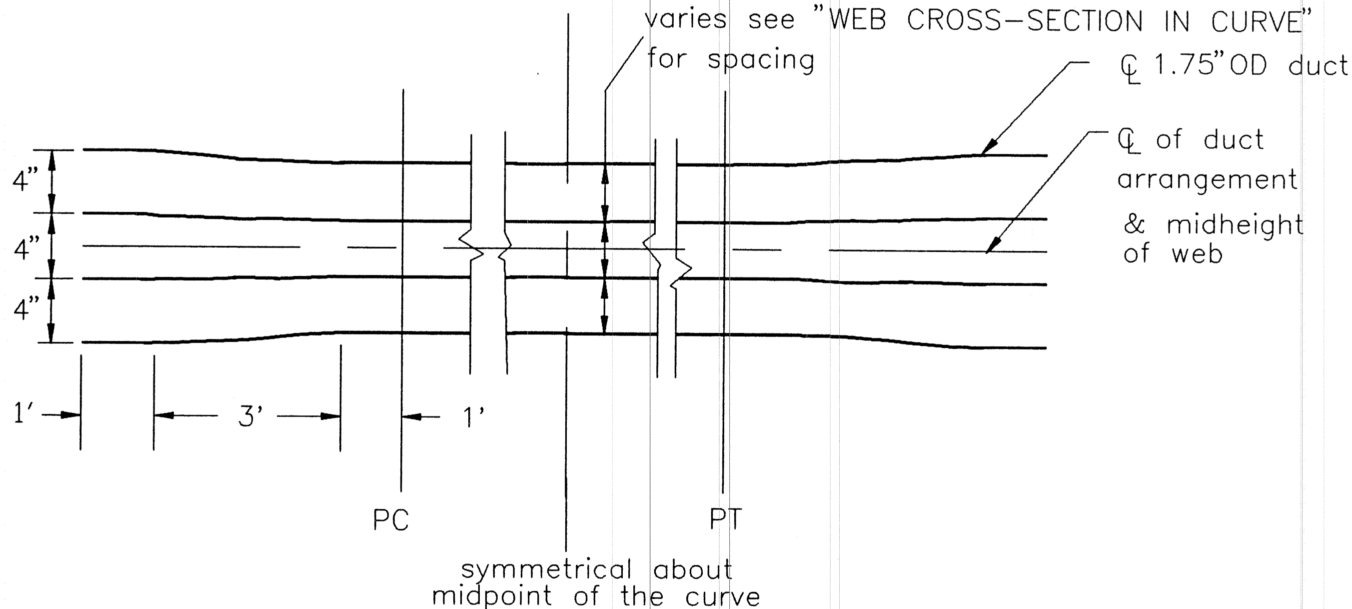

Figure 2.3 Duct Layout

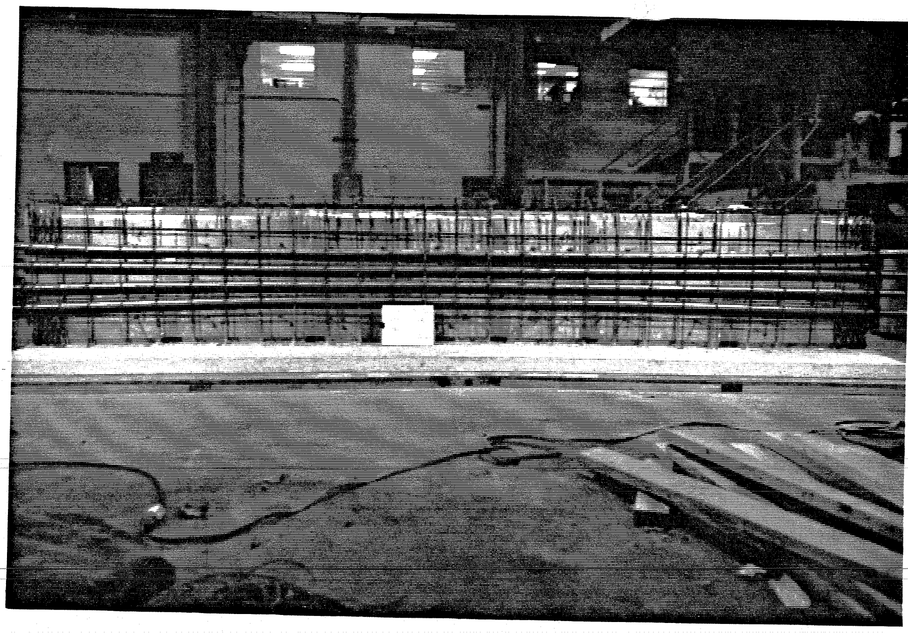

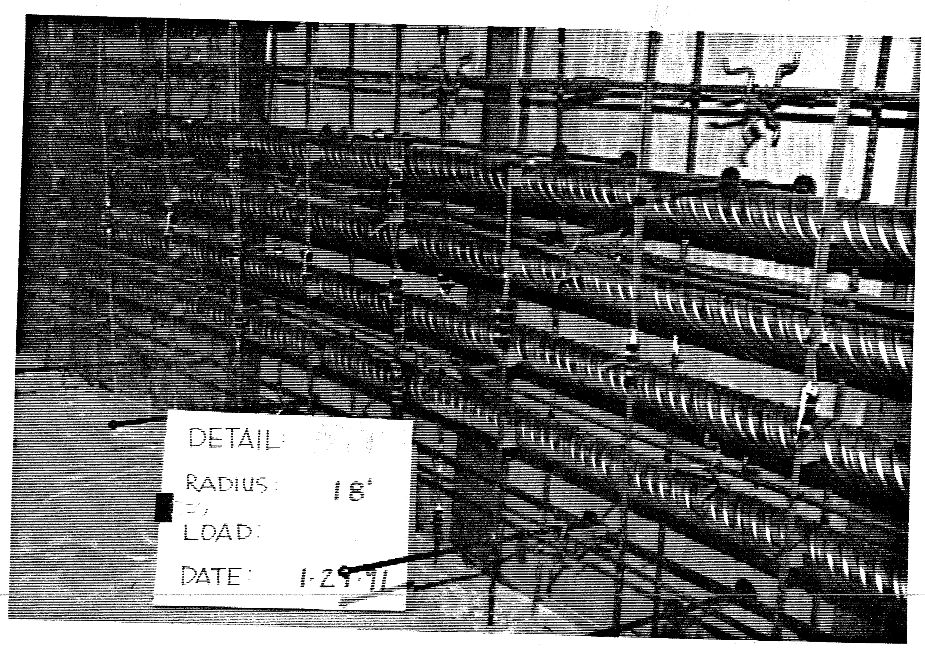

Figure 2.4 Duct Layout For Web DC

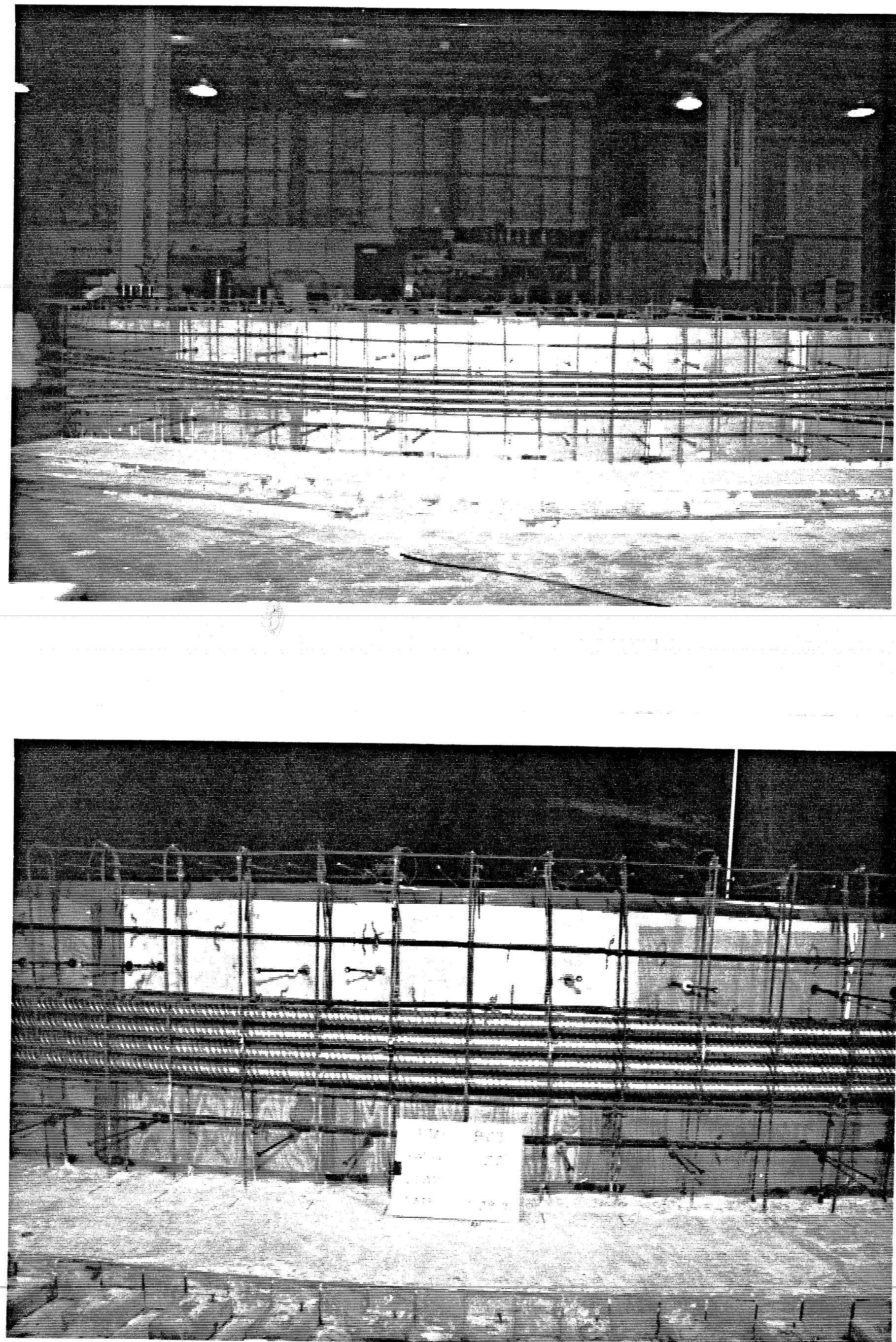

Figure 2.5 Duct Layout For Web BC

termed as BC(See Figure 2.5). The ducts at the end of both of the webs in the straight section are spaced at 4" clear. The center line of the duct arrangement in both the webs is the same as the center line of the web in elevation. Each duct carries three 1/2" strands. In all, twelve strands were used in each web.

2.2.5 Reinforcing Details: Reinforcement details of the top and bottom slab are shown in Figures 2.6 & 2.7. Reinforcement for the top and bottom slab were calculated so as to provide strength equal to the ultimate capacity of the web in bending. The reason for this was to provide the slab with sufficient strength so that it would not fail prior to the web. Reinforcing details of the web and position of ducts in the cross-section are shown in Figures 2.8 & 2.9. The reinforcement provided in the web is one third scale of that provided in the web of Las Lomas bridge. Reinforcing bars of 6mm diameter(1/3 scale of #6 bars while #5 bars were used in the Las Lomas bridge) were available in the laboratory and were used for all reinforcement required. Stirrup locations are shown in Figure 2.10. Stirrup spacing was adjusted to compensate for the use of the 6mm stirrups and to result in the correct scale of the Las Lomas bridge. Accordingly, a stirrup spacing of 7" was provided. Minimum AASHTO cover requirements for stirrups are violated as no durability problem would be expected to occur.

2.2.6 Choice of Material:

2.2.6.1 Concrete: The web concrete strength of approximately 6000 psi is representative of the strength of post-tensioned box girders during construction. Since the web section is only 4" thick, 3/8" pea gravel coarse aggregate was used in the concrete. Due to the thin web, consolidation of concrete is a problem. Superplasticizer was mixed in web and top slab concrete to increase workability and improve consolidation around the ducts in the web. The bottom slab was cast months before the web and the top slab were cast. No additive was mixed in the concrete used for the bottom slab. Coarse aggregate consisting of 3/8" pea gravel was also used in the bottom slab concrete. A local ready mix plant supplied the concrete.

2.2.6.2 Mild Reinforcing Steel;: Reinforcing steel required for the webs and the slabs had to be thin enough to meet the minimum cover and strength requirements. Grade 75 6mm Swedish bars were available in the laboratory and

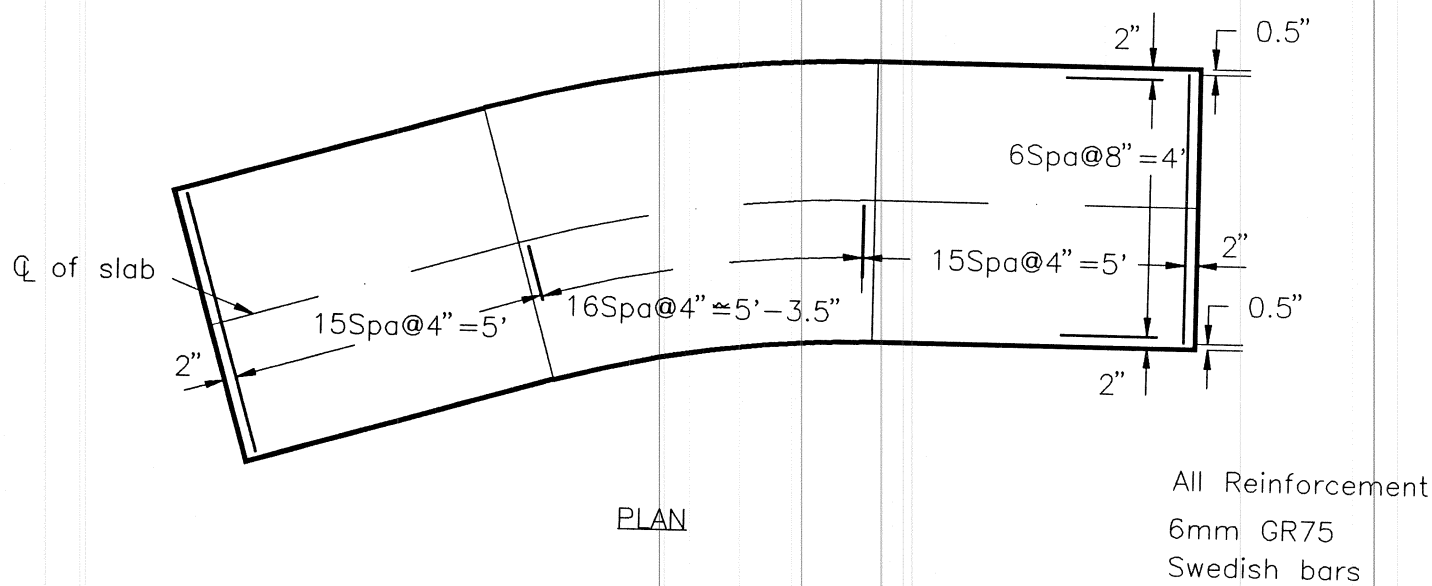

Figure 2.6 Reinforcement Details of Top Slab

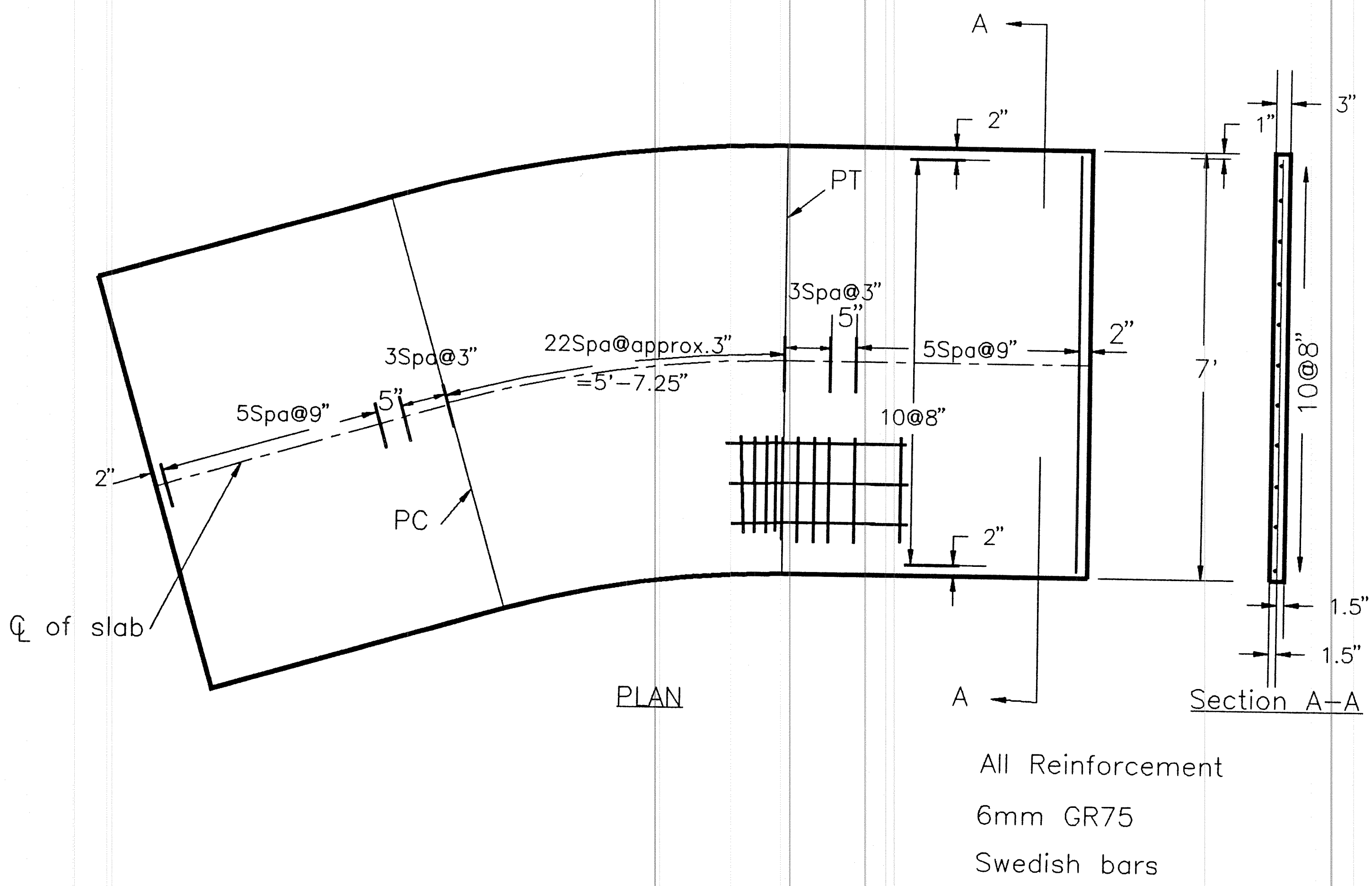

Figure 2.7 Reinforcement Details of Bottom Slab

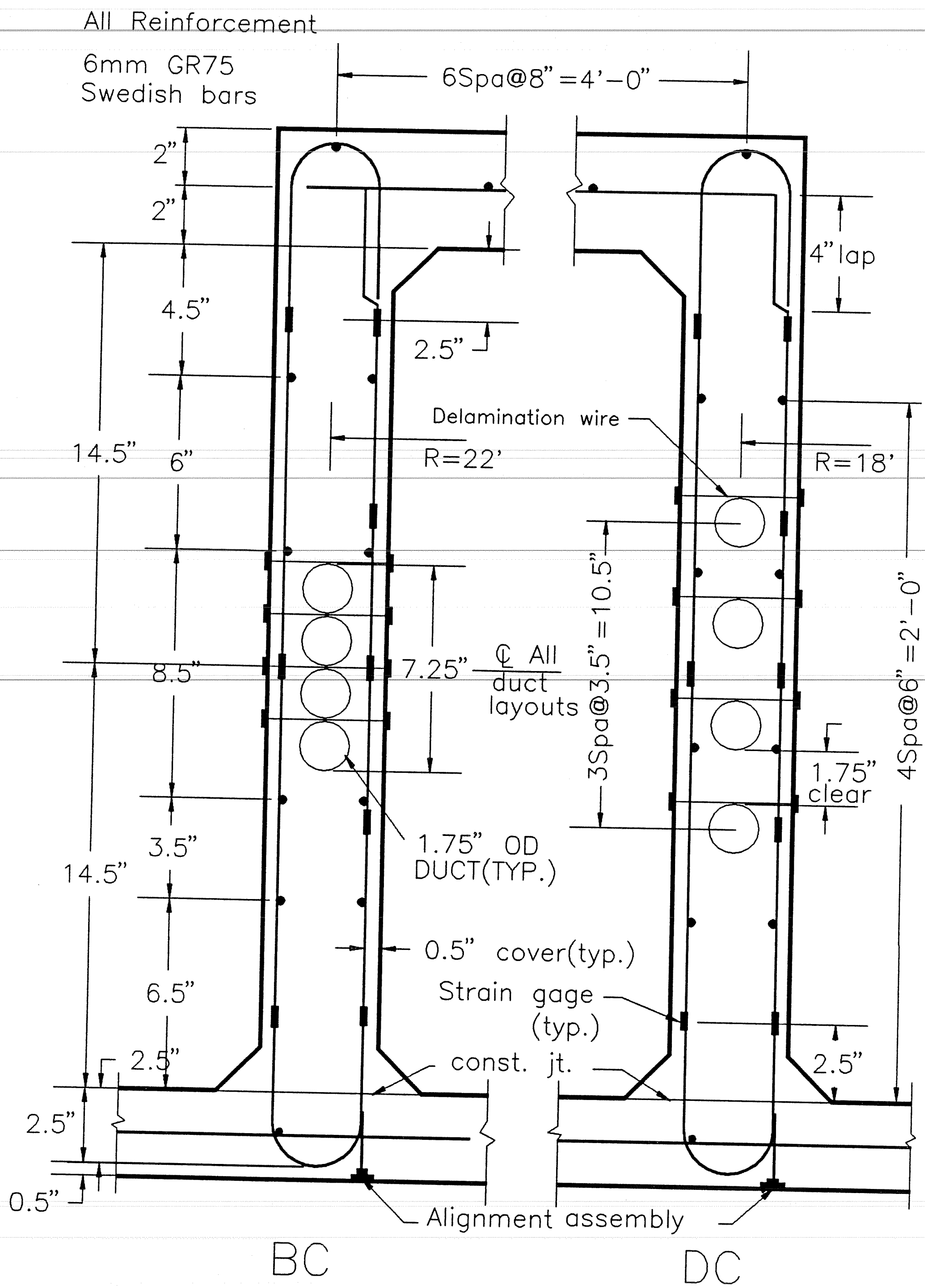

Figure 2.8 Web Cross-section in Curve

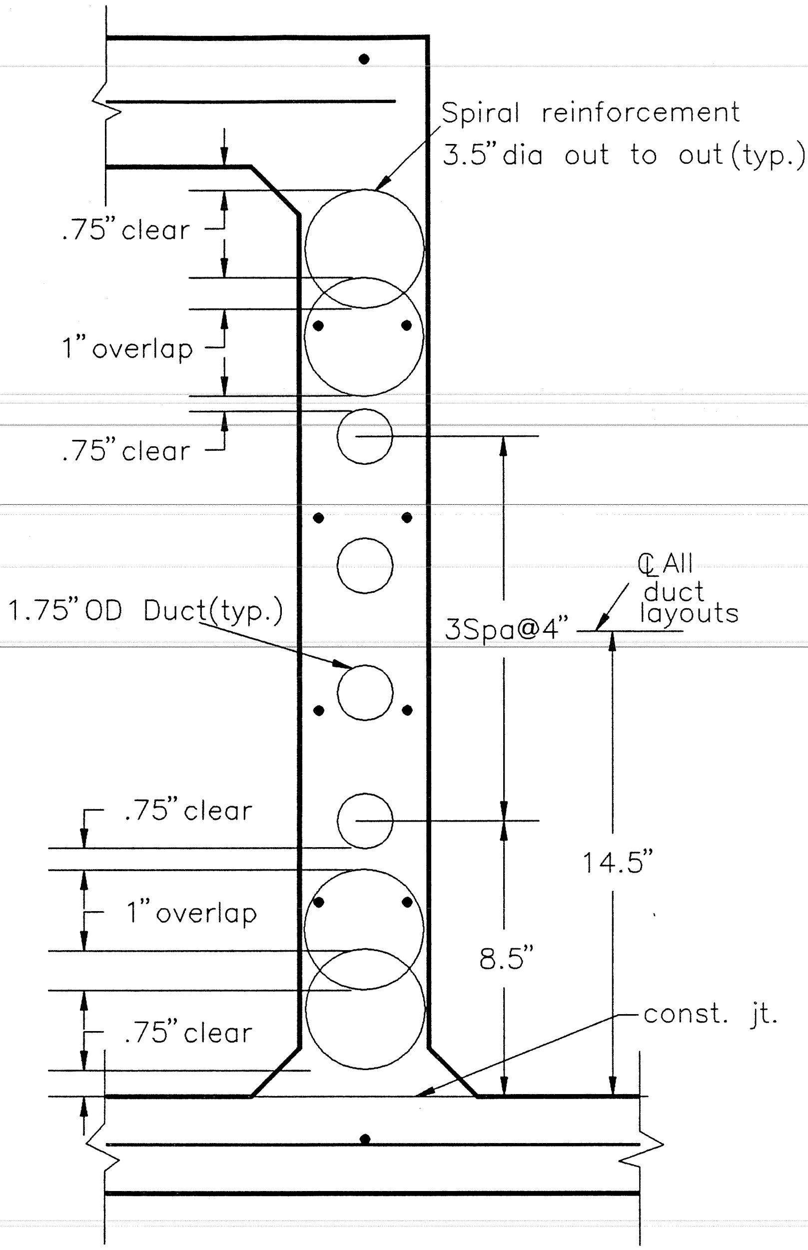

Figure 2.9 Web Cross-section at Ends

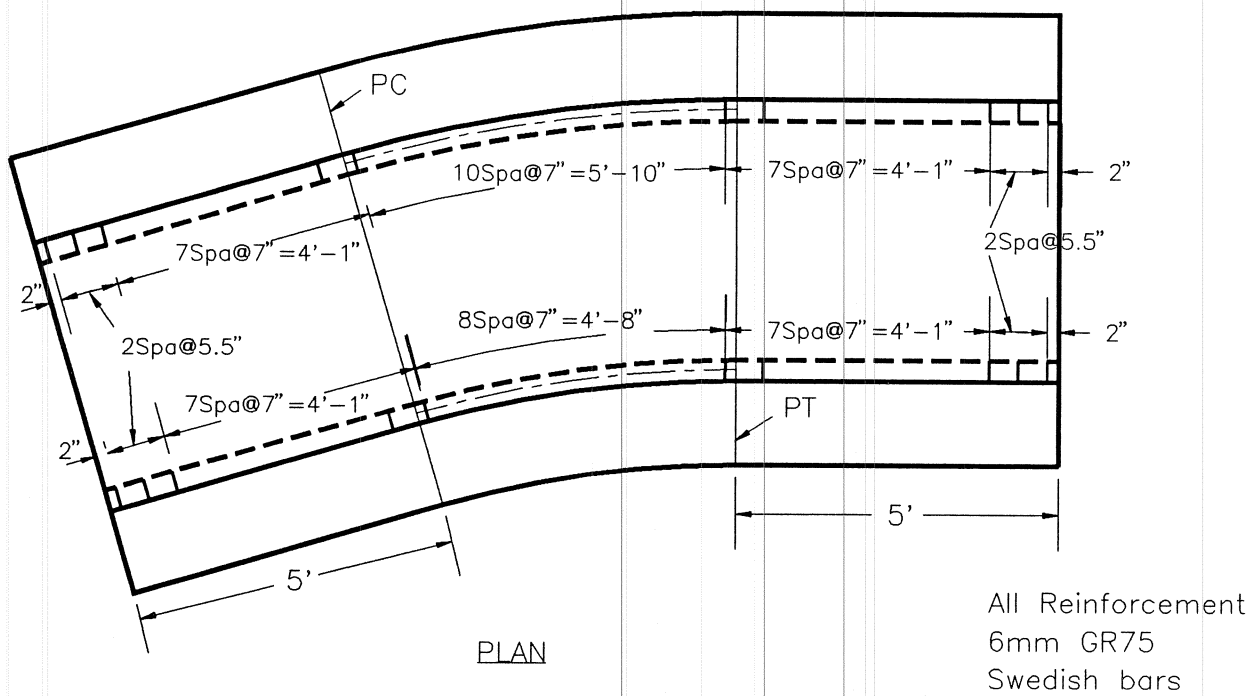

Figure 2.10 Stirrup Layout

were used to reinforce the top slab, webs, bottom slab and to make the spirals.for reinforcing anchorage zones.

2.2.6.3 Ducts: A thin wall duct with a representative scaled wall thickness was desired. Thin walled(0.035" thick, inside diameter 1.6 inch) galvanized folded metal corrugated conduit was chosen for the specimen.

2.2.6.4 Prestressing Strands: Seven wire strand with a nominal diameter of one half inch was chosen. These low relaxation strands had a nominal ultimate strength of 270 ksi. The size of the strands was compatible with the anchorage and stressing equipment used. Three 1/2" strands are placed in each duct.

2.2.6.5 Chucks: The strands were seated individually. Half inch diameter monostrand chucks were considered suitable anchorage for the strands.

2.3 Test Setup

The most important consideration in designing and building the load setup was to provide uniform loads to the web ends so as to produce a uniform stress field in the web cross-section. For this to occur all strands were stressed simultaneously. Care was taken to avoid excessive bearing pressure in the anchorage zones of the web. It is necessary that the load application to the webs be perfectly normal to its cross-section. It was also necessary to consider safety and adaptability of the testing equipment. During post-tensioning of tendons, large quantities of concentrated energy are stored in highly stressed tendons. Controlling this energy is a difficult task. Several precautions had to be taken to ensure the safety of the testing crew and the laboratory personnel in case of a brittle and explosive failure. It was important to have a test setup which is adaptable since the type of failure and the failure load cannot be foreseen. Flexibility with respect to tendon size and the number of strands per tendon is important in case any change is desired for future tests.

2.3.1 General Layout: The loading setup consisted of two heavy steel frames. The frame which transfered the reaction from the strands to the web is termed as the dead end. The frame at which the strands were stressed is termed as the live end. The dead end frame was suspended by a steel chain to a threaded round eye hook. The adjustable hook was bolted to a cantilever frame as shown in Figure 2.11. Two heavy steel chairs were welded to the dead end frame(Figure 2.12) to transfer the reaction to the web. A bearing attachment was made with two steel plates with a neoprene pad in-between the plates. This bearing attachment was used on both the live and dead ends of the specimen(Figures 2.12 & 2.14) so as to provide a uniform stress field in the web and prevent crushing of the concrete in the anchorage zone of the web. The bearing assembly took care of any possible load eccentricity due to unequal stressing or movement of the reaction/loading frame. The steel frame on the live end was suspended by a chain hoist. Two 100-ton capacity hydraulic rams provided the jacking force and pushed the live end steel frame away from the specimen. They also transfered the reactions to the web of the specimen. The top ram was suspended by tie wires to a threaded round eye hook(Figure 2.13). The adjustable hook was bolted to a cantilever frame. The top ram was also tied to the cantilever frame with duct tape for additional support. The bottom ram was placed in position by a hydraulic, forklift. The forklift was removed after the tendons were stressed to a predetermined level and the chucks were seated. The bottom ram was slightly smaller in length than the top

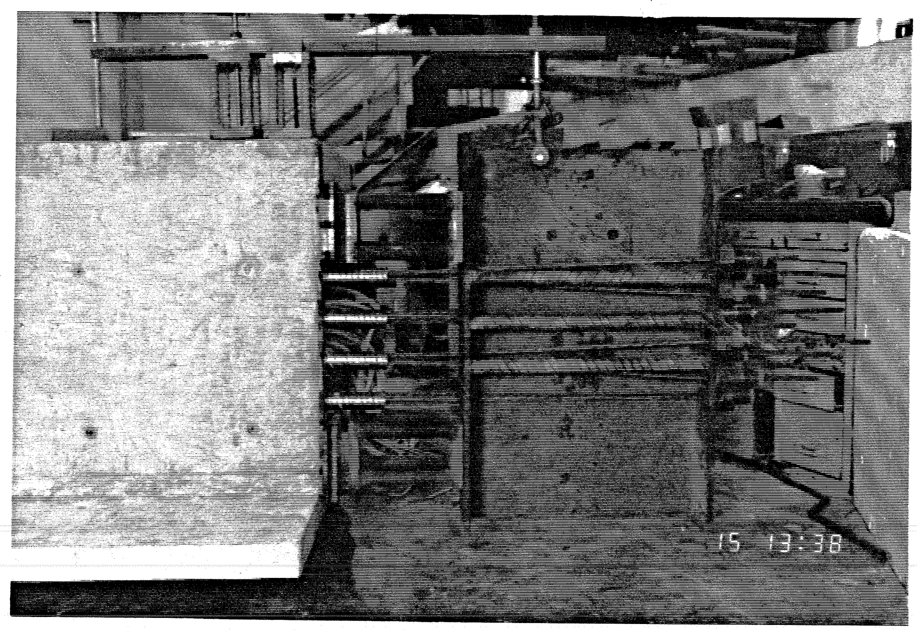

Figure 2.11 Dead End Frame

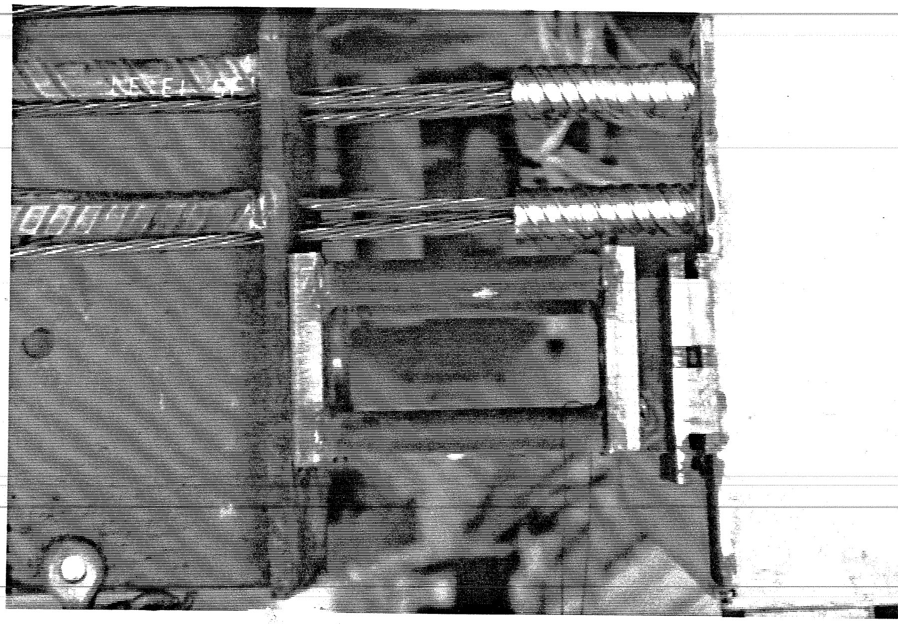

Figure 2.12 Chairs Welded to Dead End Frame

ram. Spacer plates were used between the ram and the bearing arrangement to provide a tight fit(Figure 2.14). The strands flared out between the flanges of the live and dead end frames(Figures 2.11 & 2.1.3)

Two hydraulic pumps were used with all the necessary accouterments. These pumps were used for seating the wedges with a monostrand ram, and to load the rams. An IBM AT computer and the scanner used for data acquisition were located adjacent to the pumps at the live end of the specimen. A video camera and a theodolite were installed on the southern side of the specimen to monitor and record the test. An automatic level served as an optical remote sensing device to read the dial gages.

2.3.2 Safety Features: Safety of the laboratory personnel and equipment was a prime concern during testing. Large concrete barriers were used directly behind the live and dead end steel frames. This was done to keep the tendons from flying out in case of a strand breakage or an anchorage failure. Two approximately five foot high cast iron dump carts were used as protection against

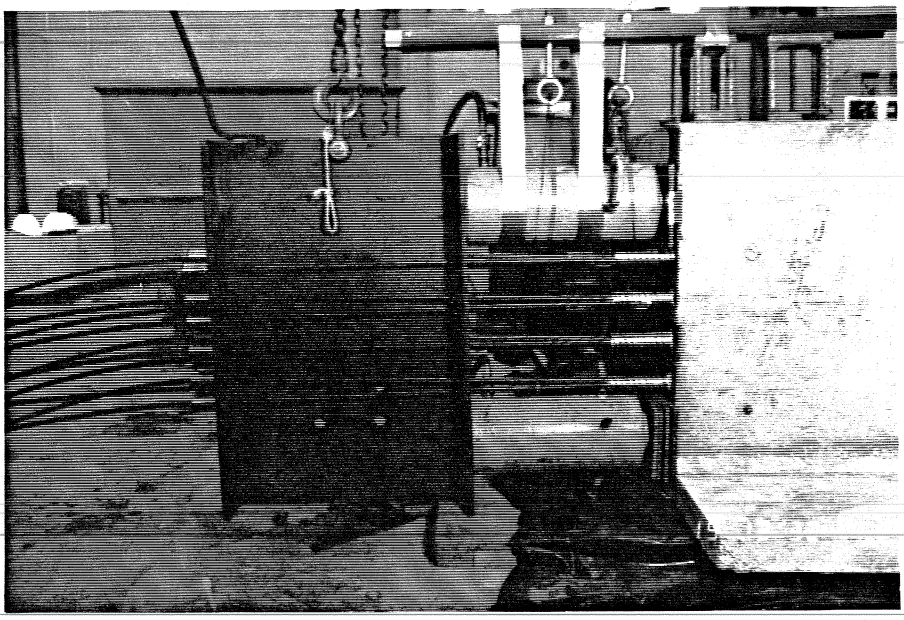

Figure 2.13 Live End Frame

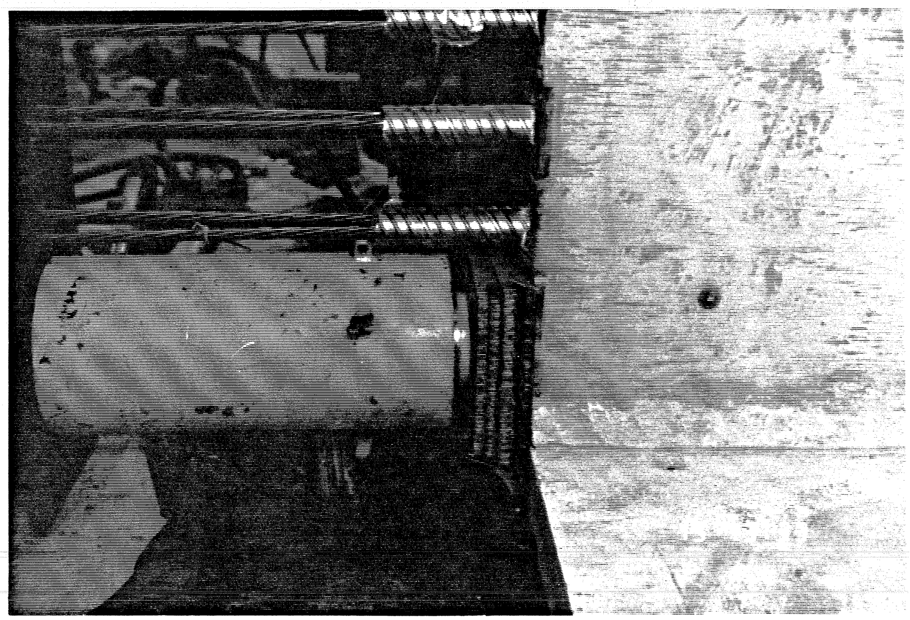

Figure 2.14 Bearing Arrangement

any projectiles. The area around the specimen was marked unsafe for other laboratory personnel during the tests. The frame at the live end was left hanging to the chain block although the chain was kept slack, even after seating the wedges. The purpose of this was to provide additional restraint and safety in case of anchorage failure or complete collapse of the loading mechanism.

2.3.3 Loading Concept: The radial forces in the curved portion of the web were applied by stressing the strands. By initially activating a monostrand ram with a hydraulic pump, each strand was stressed to a predetermined stress level. The wedges were then seated on the strands by using a secondary pump. The stressing operation of the strands was conducted starting from the bottom-most tendon and ending with the top-most tendon. After all strands were stressed to a predetermined stress level and all the wedges were seated, all strands were further stressed simultaneously by activating both the top and bottom 100-ton capacity rams. Stress in all strands was then increased simultaneously in increments controlled by the hydraulic pump. A pressure transducer connected to a switch and balance unit was used to monitor and control the pressure increments in the rams. As hydraulic pressure was applied to the rams they pushed out the steel loading frame, extending the strands. The reaction of this jacking load was transferred to the webs through the rams on the live end and through the chairs welded to the dead end loading frame.

Chapter 3
CONSTRUCTION AND MATERIAL PROPERTIES

3.1 Construction

3.1.1 Formwork Description: The formwork consisted of two basic parts, the bottom part for the bottom slab and the forms for the remaining box section. The forms were constructed of plywood and lumber(2x4's and 2x6's). The formwork for the box section can be divided into inner and outer walls of the web, and the forms for the top slab. All the forms were constructed in panels. The panels for the webs of the curved part of the specimen were also made curved. All panels were connected to each other by bolts and whaler-tie arrangement(Figure 3.1). The web forms were bolted to couplers which were cast in the bottom slab.

Figure 3.1 Form Connection

The couplers were welded to steel plates which were cast in the bottom slab. All panels were numbered and were unique in their position. The top slab forms were supported by 2x4 shores which were braced to avoid any buckling of the shores during concreting(Figure 3.2). Plywood was used to cover the web ends. All the

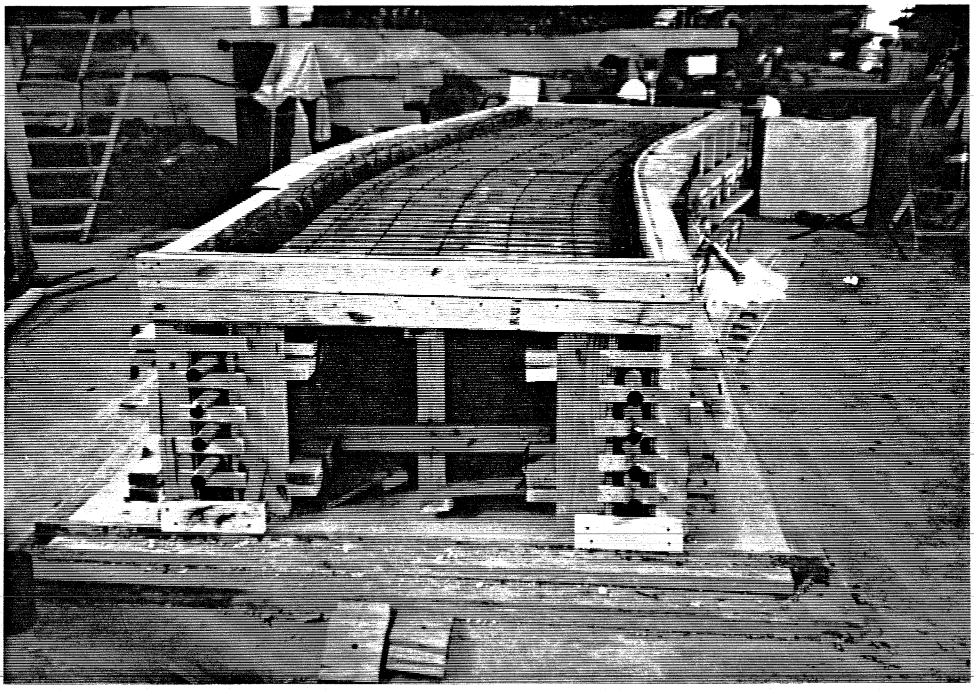

Figure 3.2 Shores Supporting Top Slab Forms

panels were constructed in such a way so that they could be assembled and disassembled with ease. Sheet metal flashing was provided on the inner side of the forms to cover 1/2" nominal joints between interior core panels. Silicone was applied at the joints from outside to prevent any leakage during concreting. To ensure reusability and facilitate stripping of forms, the forms were coated with layers of lacquer and flashing was protected with a cover of duct tape.

3.1.2 Construction of Reinforcement Cage: All mild steel reinforcement was cut using an electric band saw. The mild steel reinforcement was bent by hand in the laboratory. Dimensions were checked by comparing against one reinforcing bar cut and bent according to required dimensions. Post-tensioning strands were cut using an electric cutting disc. Spirals were made on the lathe and were tied to stirrups to reinforce the anchorage zone of the web as shown in Figure 3.3. The bottom slab steel reinforcement was laid on steel chairs to maintain proper

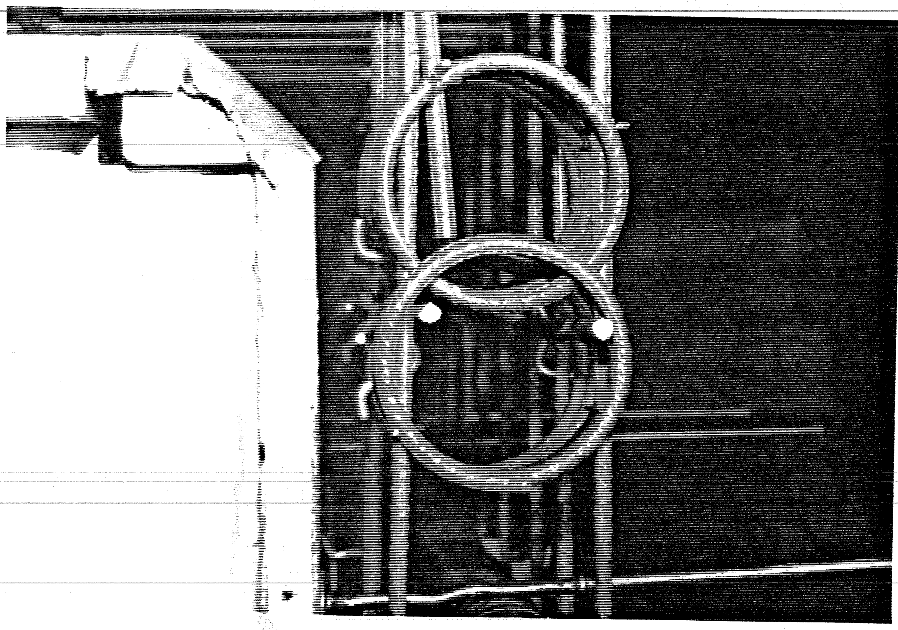

Figure 3.3 Anchorage Zone Reinforcement

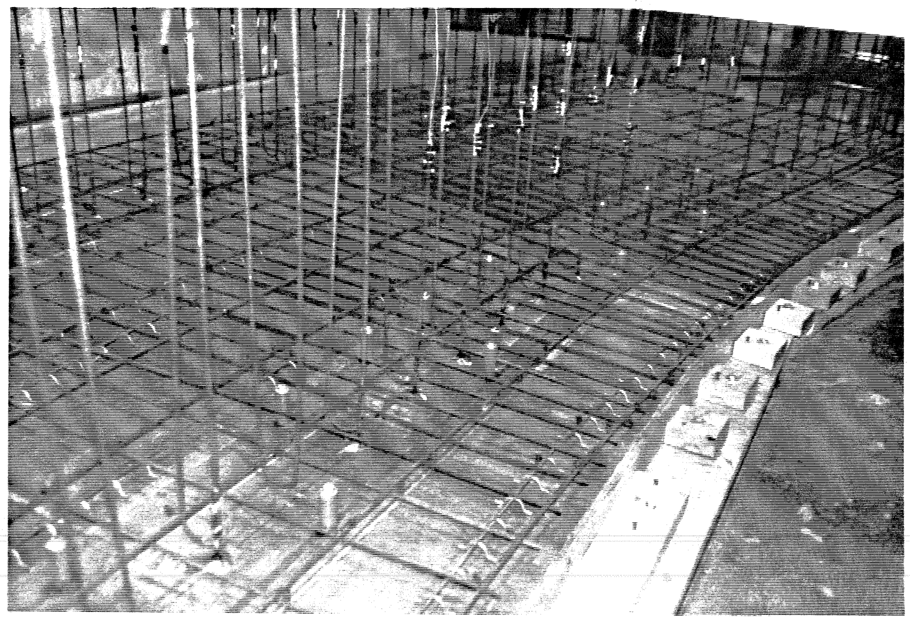

Figure 3.4 Bottom Slab Reinforcement

cover as shown in Figure 3.4. The stirrups were instrumented before being placed at proper spacing and cover in the bottom slab. Steel studs were tack welded to the stirrups which were then placed in an alignment assembly(Figures 3.5 & 2.8) to ensure the required spacing and cover of the stirrups. The alignment assembly consisted of nuts welded to a steel washer placed in the bottom slab. The alignment assembly was greased to facilitate stripping after completion of the test and ensure its reusability. Longitudinal web reinforcement and the ducts were placed in position after the bottom slab was cast. Steel chairs, plexiglass and wooden spacers

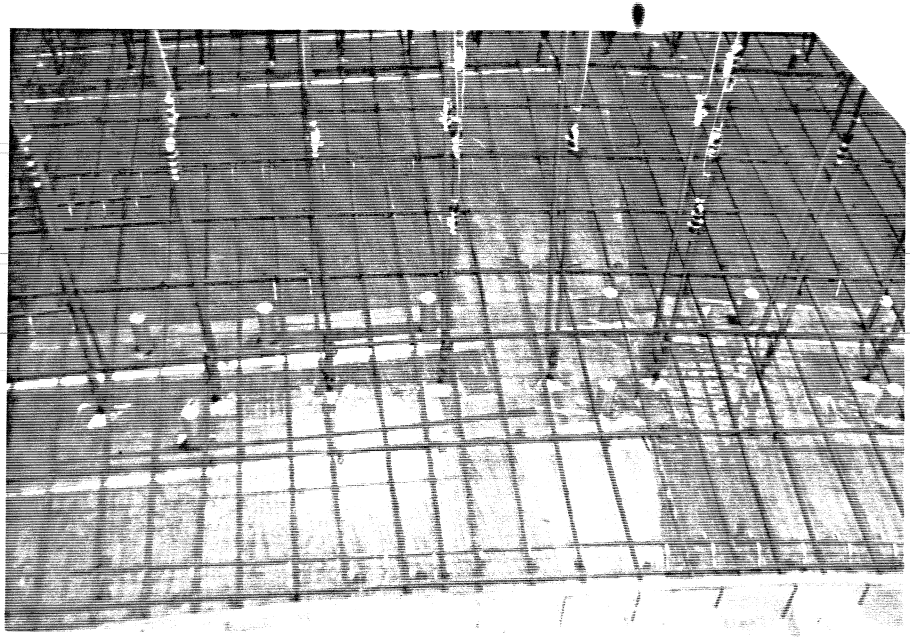

Figure 3.5 Alignment Assembly

were used to maintain the correct cover and position of the ducts(Figure 3.6). Top slab reinforcement was placed in position after the web formwork and top slab panels were placed in position(Figures 3.7 & 3.8). Holes were drilled in the web formwork to slide 1/8" outer diameter plastic tubes in the web just above the duct position. These tubes were required to make cylindrical cavities in the web to place the delamination gage wire(Figure 3.9).

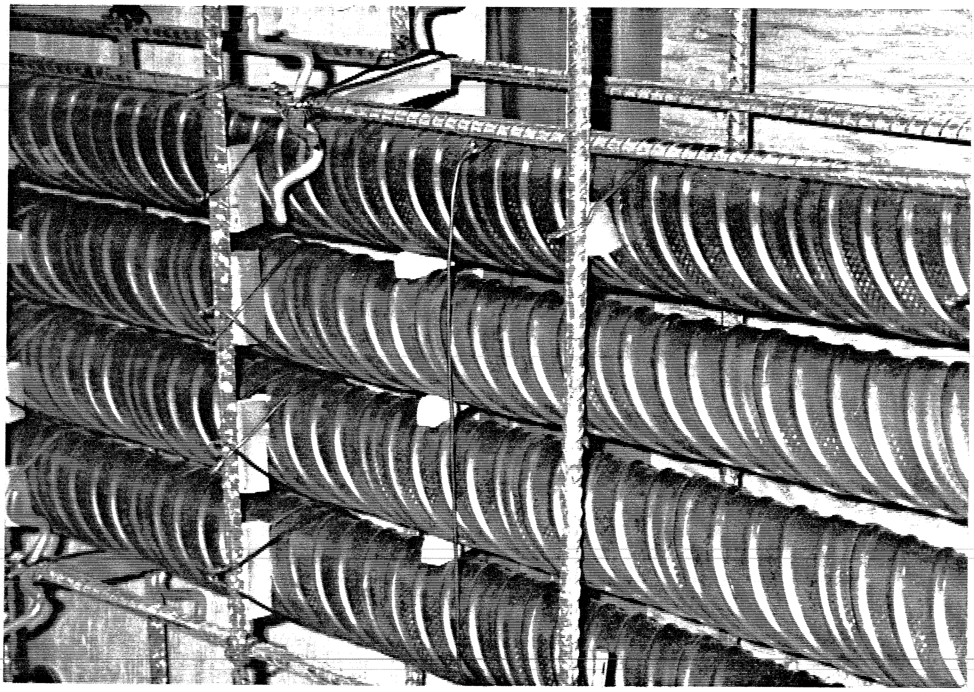

Figure 3.6 Spacers Used to Maintain Cover

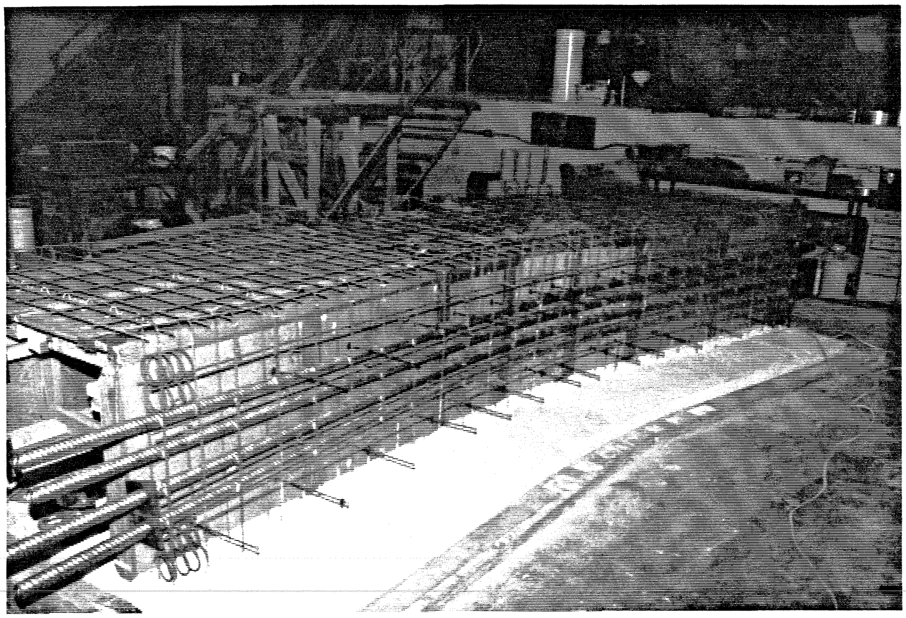

Figure 3.7 Web & Top Slab Reinforcement

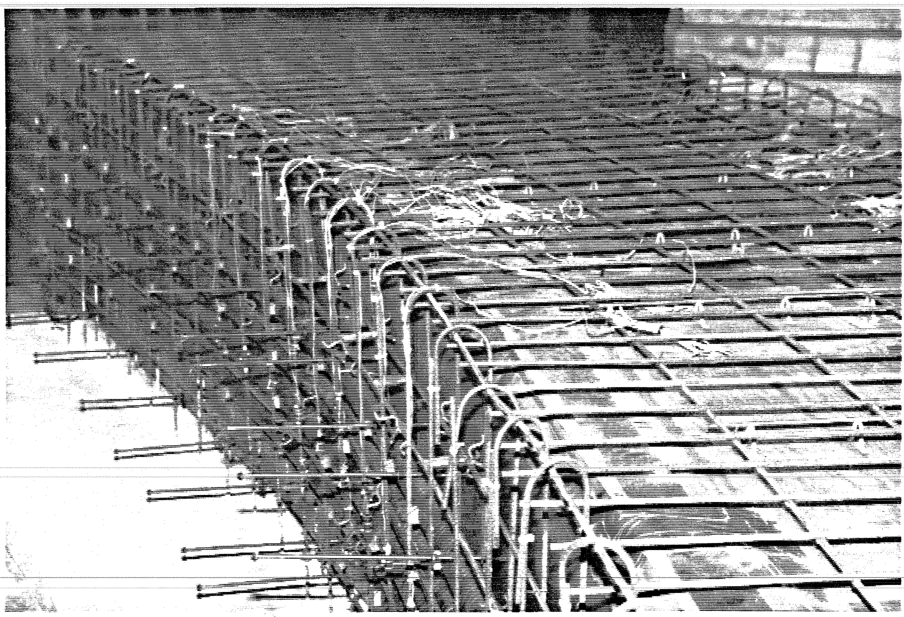

Figure 3.8 Top Slab Reinforcement

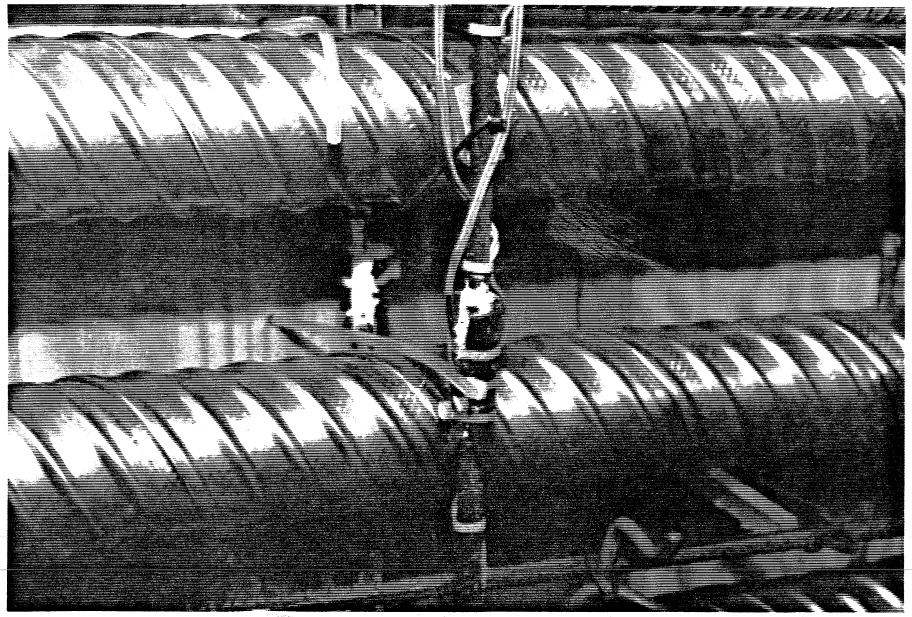

Figure 3.9 Delamination Gage Tubes

3.1.3 Instrumentation of Stirrups: Strain gages were used to monitor strains in stirrups. The strain gages were affixed on the face of stirrups facing the web cross-section as shown in Figure 3.10. It is required to have a fine

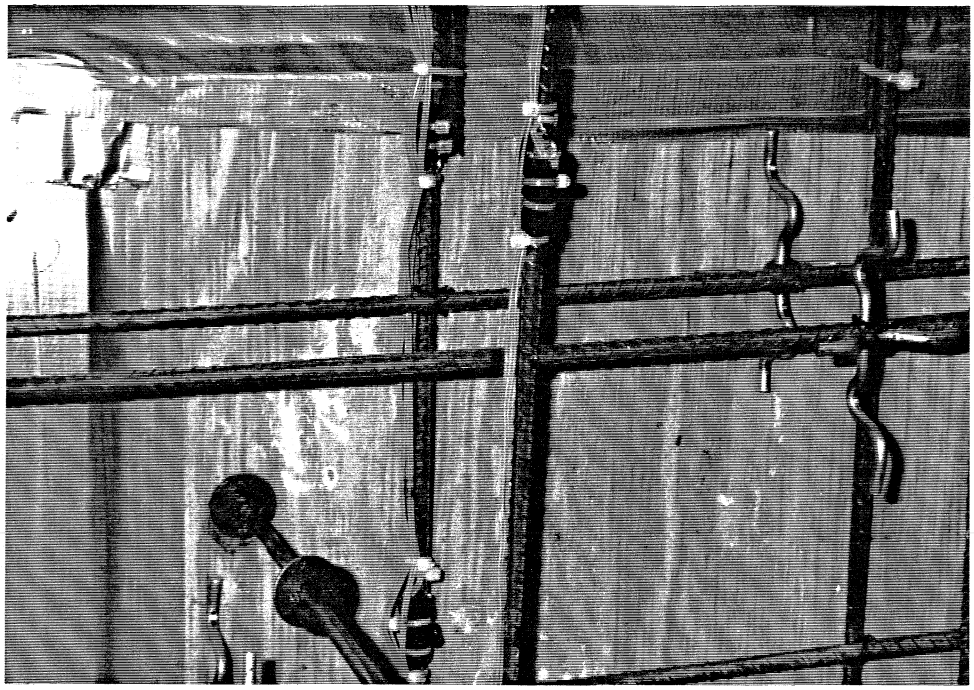

Figure 3.10 Position of Strain Gage

clean smooth surface on the bars for the strain gages to adhere on the bar surface. A pneumatic hand grinder was used to remove the deformations of reinforcing bars at the required locations on the bar. The bars were further smoothened by hand sanding using a fine grit sand paper. Care was taken to avoid any unnecessary reduction in bar area. The smooth surface was then cleaned with acetone and then treated with an acid, which was subsequently neutralized by a base. The surface was then wiped dry. A glueing catalyst was applied on the strain gage which was then affixed on the bars using a high strength adhesive. The gage was then coated with a white waterproof acrylic coating. A piece of butyl rubber(self affixing) was stuck on the strain gage to protect it from any abrasion during concreting. The rubber was painted with the white insulating acrylic coating. The strain gage was then wrapped with a thin layer of neoprene rubber to provide further protection during concreting. The lead wires were tied to the stirrups by plastic ties to prevent them from tearing off during concrete placement and vibration.

3.1.4 Concreting: Concreting was done in two stages. The bottom slab was cast in the first stage and the webs and top slab were cast in the second stage. Figure 3.11 illustrates the bottom slab just after it was cast with the stirrups in position. The slump of concrete used for casting the bottom slab was 3.5 inches. Fresh concrete was placed using a bucket which was lifted by an overhead crane. One inch diameter vibrators were used to consolidate the concrete. Screeding was done longitudinally with a long aluminum screed.

Figure 3.11 Bottom Slab

In the second stage three yards of ready mix concrete was received at a 2 inch slump. Superplasticizer was added to the concrete to improve its workability. The slump after the addition of the admixture was 7 inches. The slump immediately after concreting the top slab(approximately an hour after superplasticizer was added) was 4 inches. Hand scoops were used to place concrete in the webs. Web concrete was placed in three lifts. To prevent any honeycombing, each layer of concrete was tamped with 6mm reinforcing bars. The placing operation is shown in Figure 3.12. Mild steel bars(1.5"x3/8"x36") were clamped to half inch diameter vibrators(Figure 3.13), so that they could be inserted all the way

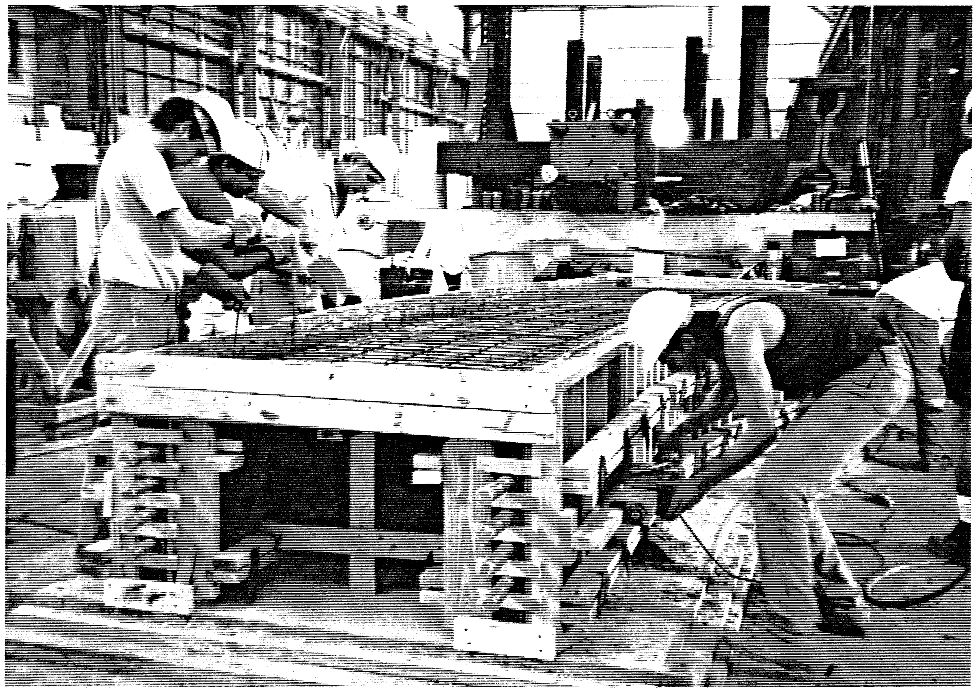

Figure 3.12 Concreting Operation

down in the web. Form vibrators were also used for proper consolidation of concrete. Concrete in the top slab was placed using a bucket which was lifted and moved by an overhead gantry crane. Screeding of the top slab was performed transversely using an aluminum screed(Figure 3.14). Several test cylinders were cast for both first and the second stage placements.

3.1.5 Curing: After finishing, the specimen was covered with wet burlap and was enclosed in a layer of plastic sheeting. The forms were stripped after twenty four hours and the moist curing of the anchorage zones in the web was

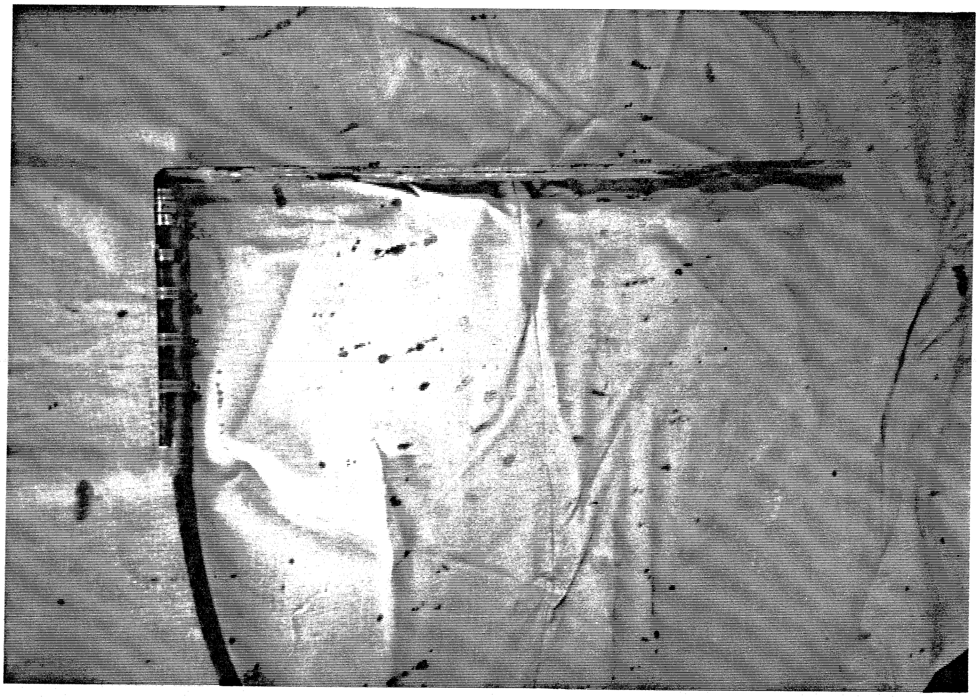

Figure 3.13 Metal Bar Vibrator

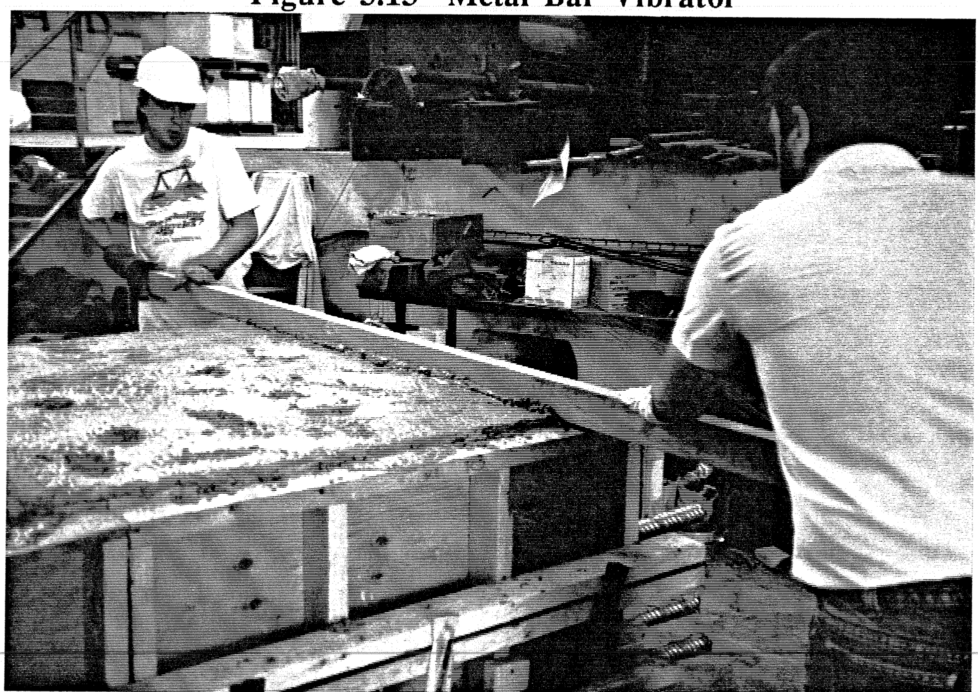

Figure 3.14 Screeding Operation

continued for three days. Test cylinders were cured in the same fashion as the specimen.

3.1.6 Dimensions after Construction: Measurements of the web thickness just after specimen construction and the stirrup cover measured after web failure is shown in the Table 3.1.

	Web Thickness				Stirrup Cover			
	Designed	Measured			Designed	Measured		
		Max.	Min.	Mean		Max.	Min.	Mean
Web DC	4.00"	4.06"	3.94"	4.00"	0.5"	0.56"	0.38"	0.47"
Web BC	4.00"	4.13"	3.94"	4.00"	0.5"	0.5"	0.47"	0.48"

Table 3.1 Critical Dimensions

3.2 Material Properties:

3.2.1 Concrete: The mix proportions of concrete as received from the premix plant are shown in Table 3.2. 14.84 lb of Relcrete M150 superplasticizer was mixed with the three yards of concrete used to cast the web and the top slab.

	Material Quantities(per cubic yard of concrete) as batched	
	Top Slab and Web	Bottom Slab
Cement(Type I)	512.67 lb.	536 lb.
Fine Aggregate	1691.7 lb.(4.97% moisture)	1573.4 lb.(5.53% moisture)
Coarse Aggregate	1621.67 lb.	1625 lb.
Water	20.83 gl.	8 gl.

Table 3.2 Concrete Mix Proportion

Concrete cylinders were tested for compressive strength under uniaxial compression at various important ages. The variation of compressive strength of concrete with age is shown in Figure 3.15.The strength of web concrete at the time of the tests were 5951 psi(15 days after casting) and 5984 psi(27 days after casting). Bottom slab strength was 5365 psi on the day of the second test(147 days after pouring).

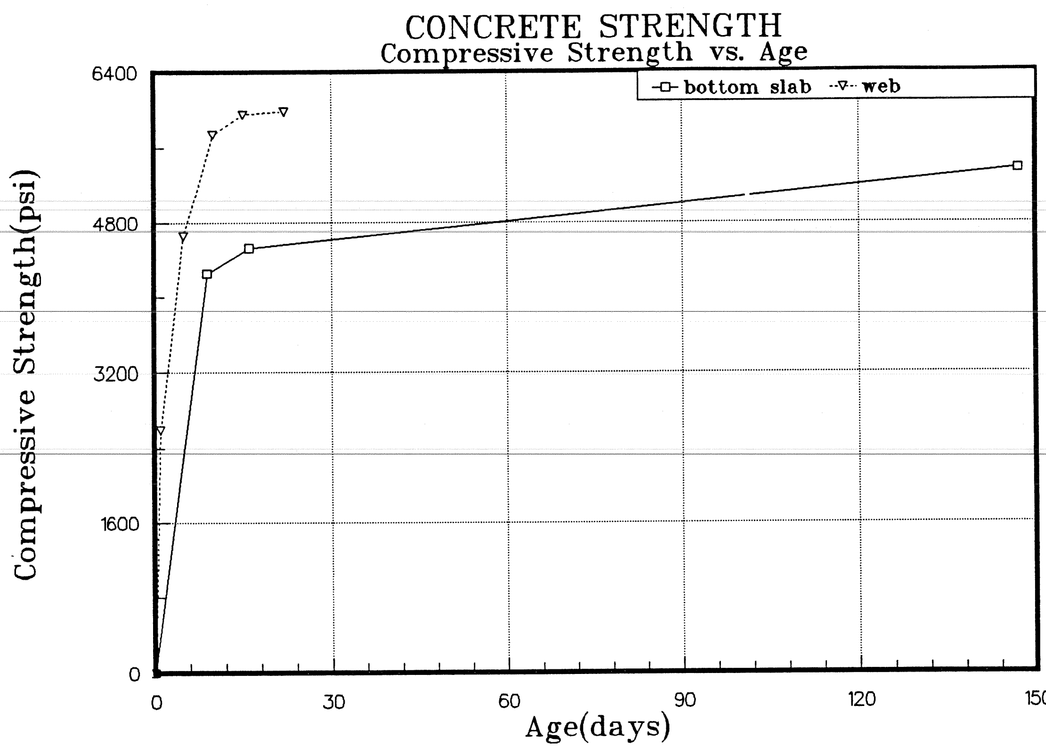

Figure 3.15 Concrete Strength Vs Age

3.2.2 Mild Steel Reinforcement: 6mm diameter hot rolled deformed bars(equivalent to #2 bars in the United States sizing system) Swedish bars were used for all reinforcement purposes. Specified mill yield strength was 75 ksi. These bars were used in a test program described in Reference 6. Results of detailed tests conducted on these bars are given in that reference.

3.3.3 Prestressing Strand: The prestressing strand used in this test program is a seven wire, low-relaxation strand and has a nominal diameter of one half inch(area = 0.153 square inches). The strand has a specified ultimate strength of 270 ksi. The manufacturer's(Florida Wire And Cable Company) data specifies a yield stress of 276 ksi and an ultimate stress of 289.5 ksi. These strands were used in a test program described in Reference 7.

3.3.4 Prestressing Duct: Galvanized corrugated folded metal ducts were used in this test program. The outer diameter of the ducts measured ridge to ridge is 1.75 inch and the inner diameter measured valley to valley is 1.6 inch. The thickness of the duct metal is 0.035 inch.

Chapter 4
INSTRUMENTATION AND TESTING

4.1 Instrumentation Objectives

The prime objectives of the instrumentation were as follows:

1) To measure and control the jacking force applied by the hydraulic rams.

2) To measure the strains at various location on the mild steel stirrups in the webs.

3) To measure deflection of the web relative to the top and bottom slab, and also with respect to the web at the point of curvature and at point of tangency.

4) To measure top and bottom slab rotations.

5) To measure web concrete delamination.

6) To store all the data for further analysis and use.

4.2 Instrumentation Devices

Several electronic and mechanical measuring instruments were used. The instrumentation location and description is discussed in this section.

4.2.1 Strain Gages: Resistance type strain gages made of constantan (type FLA - 5 - 3L - 11, Tokyo Sokki Kenkyojo Co.) were used to measure strains in the reinforcing steel as well as the tendon strands. The strain gages have a gage length of 5mm, gage factor of 2.12 and a resistance of 120.3 ± 5 ohms.

Nine stirrups were gaged in the inner web(R=18', DC) and eleven stirrups in the outer web(R=22', BC). The strain gages used in each web are shown in Table 4.1. The strain gages are named on the basis of stirrup number on which they are affixed and the position on the stirrup. The nomenclature used is illustrated in Figure 4.1.

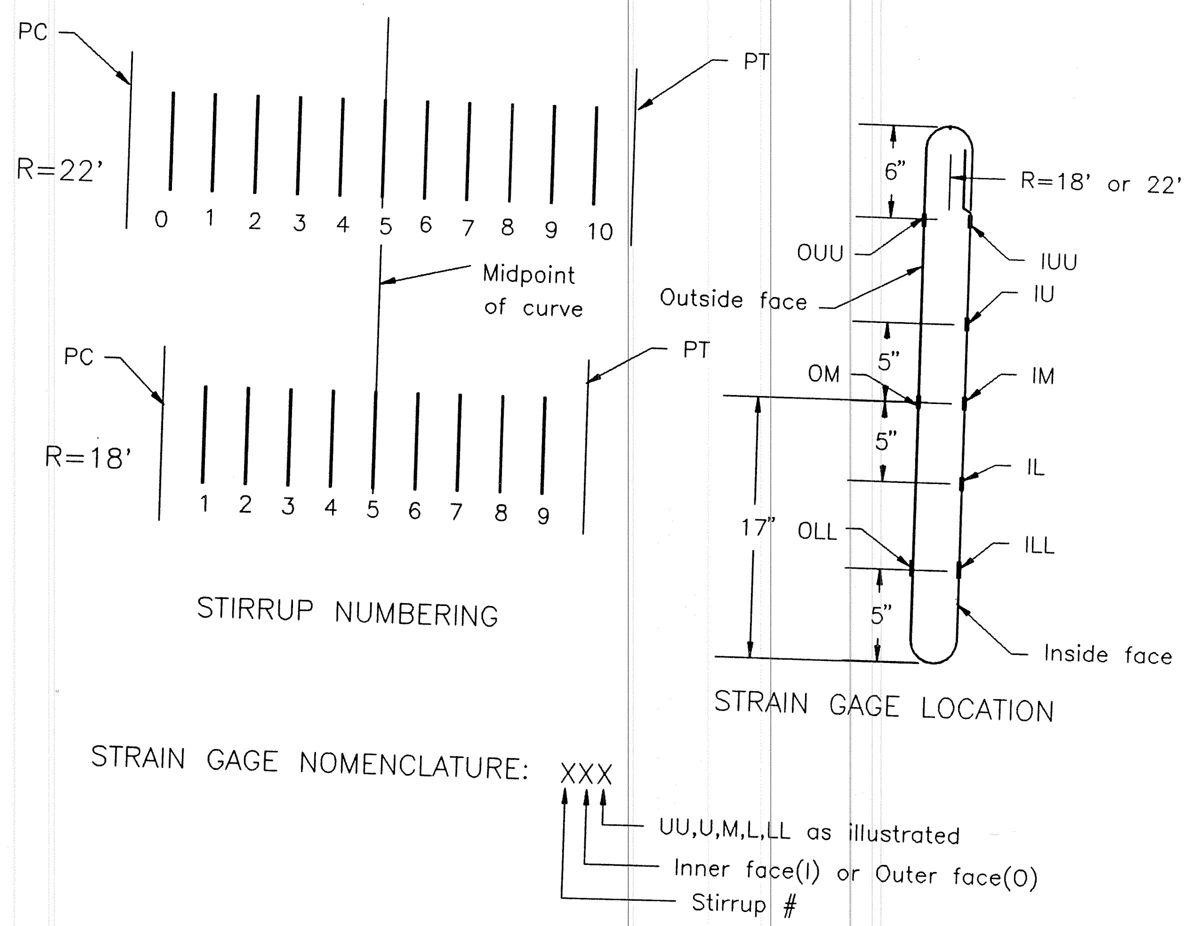

Figure 4.1 Strain Gage Nomenclature

Stirrup#	IUU	IU	IM	IL	ILL	OUU	OM	OLL
Web DC								
1			Y					
2			Y				N	
3			Y					
4		Y	Y	Y			N	
5			Y					
6		Y	Y	Y		Y	N	N
7			N					
8			Y				N	
9			Y					
Web BC								
0			Y					
1			Y					
2			Y				N	
3			Y					
4		Y	Y	Y			N	
5			Y					
6		Y	Y	Y		Y	N	N
7			Y					
8			Y				N	
9			Y					
10			Y					

Y-Strain gage installed and worked

N-Strain gage installed but did not work

Table 4.1 Inventory of Strain Gages

4.2.2 Potentiometers and Dial Gages: Four 2 inch potentiometers were used on both of the webs to measure the deflection at mid-height of the web with respect to the top and bottom slab as shown in Figure 4.2. Glass plates were glued to the web to provide a smooth bearing surface for the stem of the potentiometer. A dial gage acted as an analog back up system for the potentiometers on both of the webs. The dial gage and the potentiometers were clamped to #5 reinforcing bar which was bolted to the top and bottom of the web as shown in Figure 4.2. In the case of web BC three more potentiometers were used to measure web deflections at mid height with respect to the web at the point of curvature(PC) and point of tangency(PT). The potentiometers were clamped to a #5 reinforcing bar which was screwed to the mid height of the web at PC and PT of the curve as shown in Figure 4.5. In both of the webs the potentiometers and the dial gages were installed on the outer side of the curve. The nomenclature used is illustrated in Figures 4.3 and 4.4.

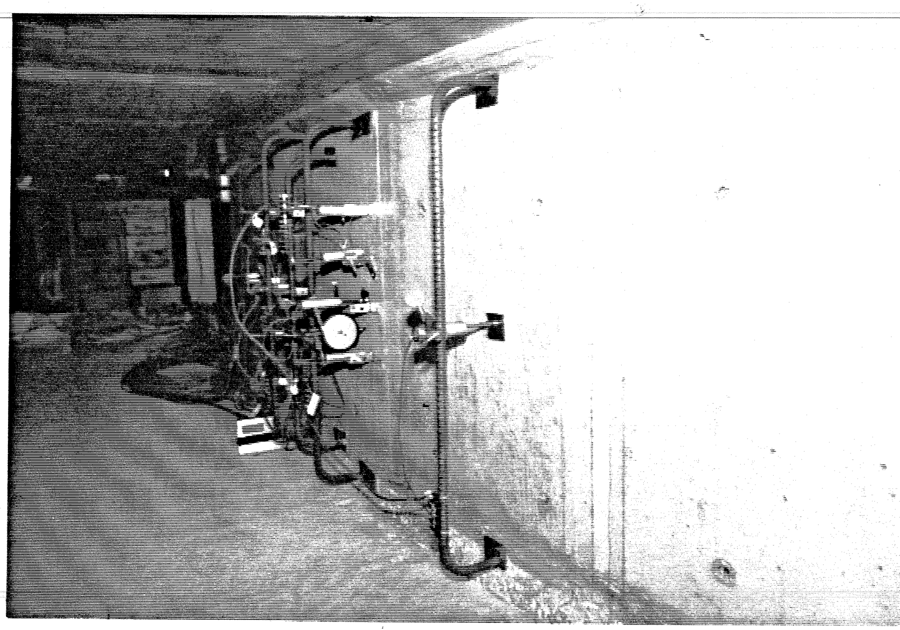

Figure 4.2 Potentiometers and Dial Gage

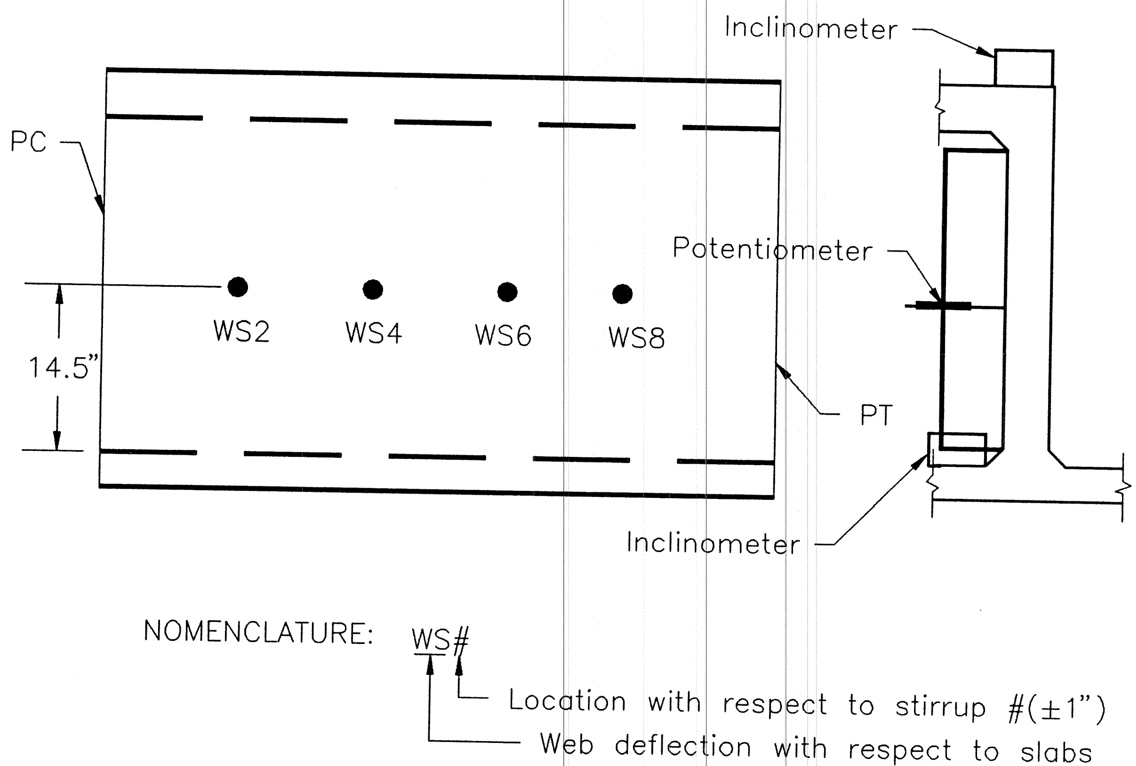

Figure 4.3 Instrumentation to Measure Web Deflections Relative to Slab

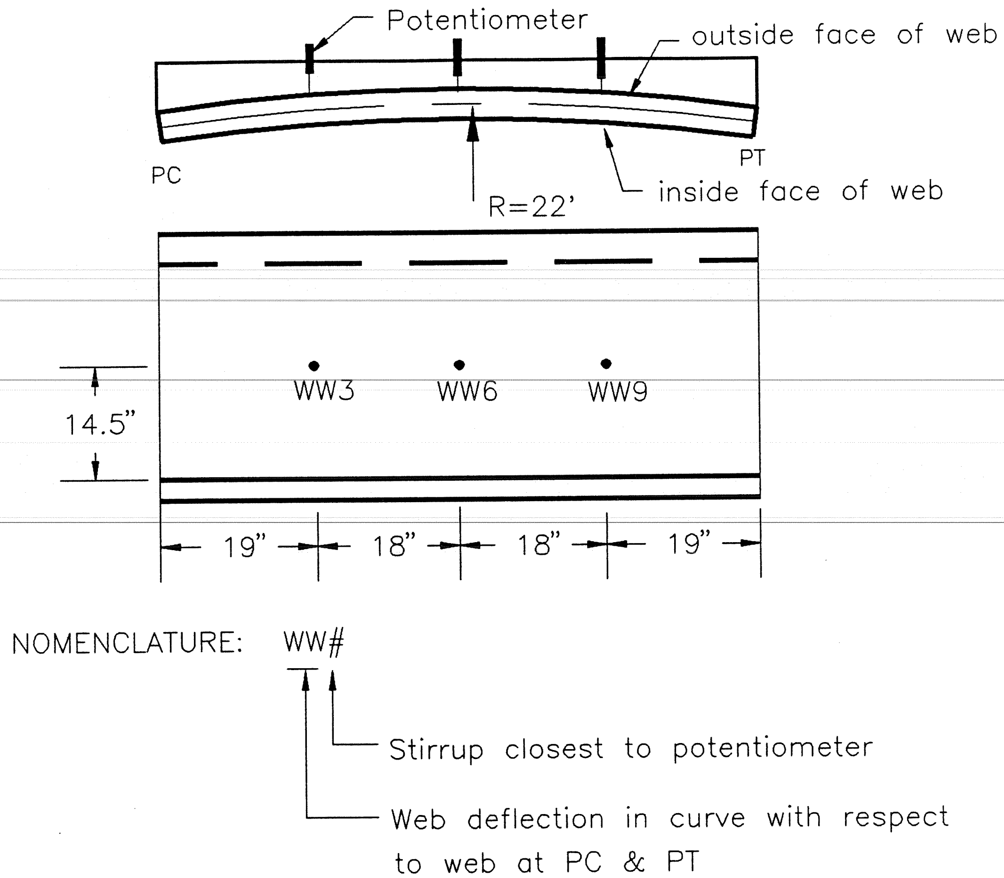

Figure 4.4 Instrumentation to Measure Web Deflections Relative to Web

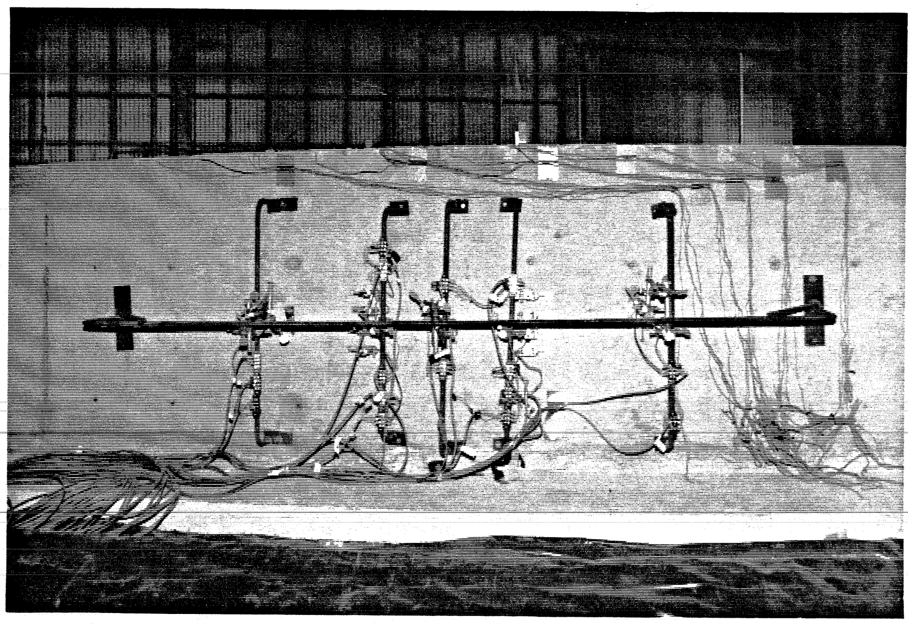

Figure 4.5 Potentiometers to Measure Deflections Relative to Web

4.2.3 Pressure Transducer and Pressure Gage: One pressure transducer was used to measure the pressure in the hydraulic circuit and to record the total pressure applied to both the rams. The pressure transducer had a capacity of 10,000 psi and 10mv/v output. The rated accuracy of the pressure transducer is 1.5 percent. An analog pressure gage was used as a back up for the pressure transducer. In all, two 10,000 psi capacity pressure gages were used. The rated accuracy of the pressure gage is $\pm$ 0.25 percent. These pressure gages were used to monitor the load while stressing the strands individually and to monitor the seating pressure during the seating operation of the wedges. The same number of pressure transducers and pressure gages were used in both the tests.

4.2.4 Demec Gages: Demec points for use with a mechanical demec gage were installed before the second test(web BC) in an effort to record any arching of the web due to jacking force applied from the ends. Five sets of demec points were installed. All demec gages were applied at the midpoint of the curve. These points were glued at the top and bottom slab on the inside of the curve of web DC and the outside of the curve of web BC. The other set of points was located at mid-height of the web BC. All gages were oriented such that they measured longitudinal movements. Each division on the demec gage corresponds to 8.1 microstrains. A demec gage was then placed on these demec points at each load stage to monitor expansions and contractions.

4.2.5 Inclinometers: Inclinometers were installed at the top and bottom slab at midpoint of the curve as shown in Figures 4.4 and 4.5 to record the rotations of the top and bottom slabs.

4.2.6 Delamination Gage: The purpose of this instrumentation was to record the movement of the inside vertical face of the concrete web with respect to the outside vertical face. A thin delamination wire of 1/8 inch diameter was passed through a cavity cast in the concrete web. On the inside face of the web the delamination wire was soldered to a piece of sheet metal which was then glued to the concrete surface(Figure 4.6). On the outside of the curve the delamination wire was tied to the stem of a two inch potentiometer with plastic ties. The potentiometer was clamped to the web surface(Figure 4.7). As the web faces moved away from one other, the delamination wire compressed the stem of the potentiometer. The relative movement of one face with respect to the other was measured as the displacement of the potentiometer stem. The delamination wires were placed just above the ducts in the cross-sections of both webs. The position of the delamination wire and potentiometers with the explanation of nomenclature is illustrated in Figure 4.8.

4.2.7 Data Acquisition System: Data from the strain gages, potentiometers and the pressure transducer was fed to a Hewlett - Packard scanner which was connected to an IBM AT personal computer. The scanner supplied an input voltage of ten volts across full bridge connections(pressure transducer and potentiometers), and two volts across quarter bridge connections(strain gages). The scanning process was controlled by a Hewlett - Packard program called HPDAS which runs on the computer. The computer also stored all the instrumentation data

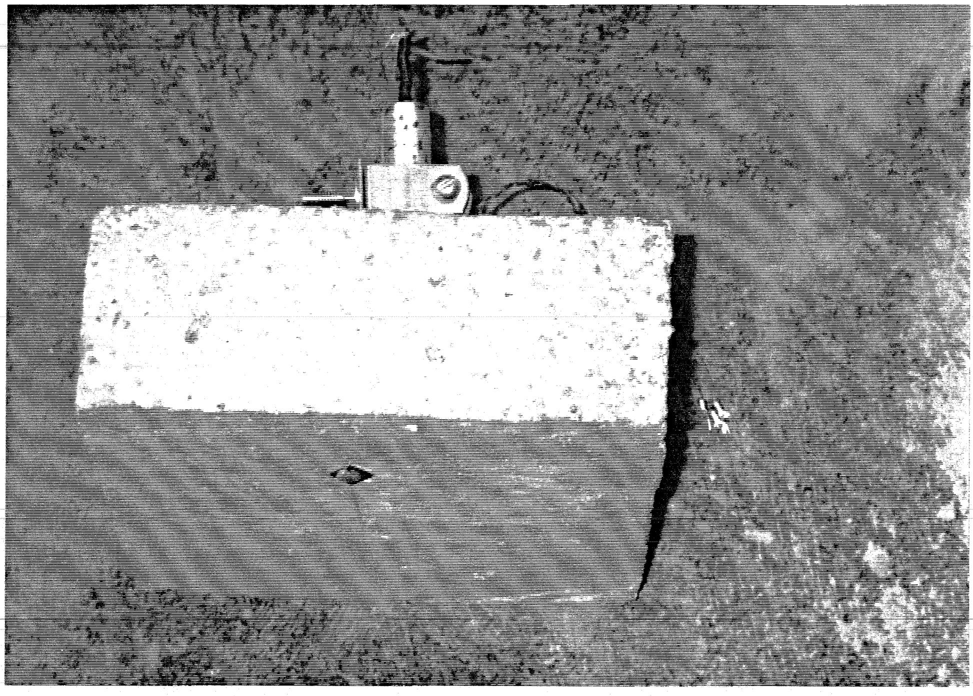

Figure 4.6 Sheet Metal Anchor

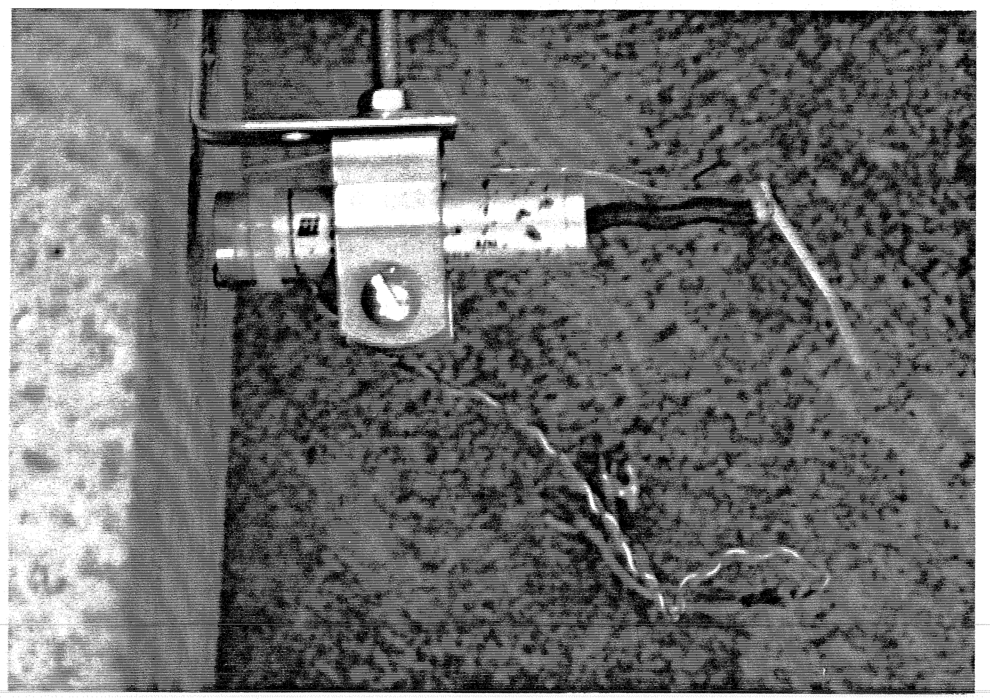

Figure 4.7 Delamination Gage

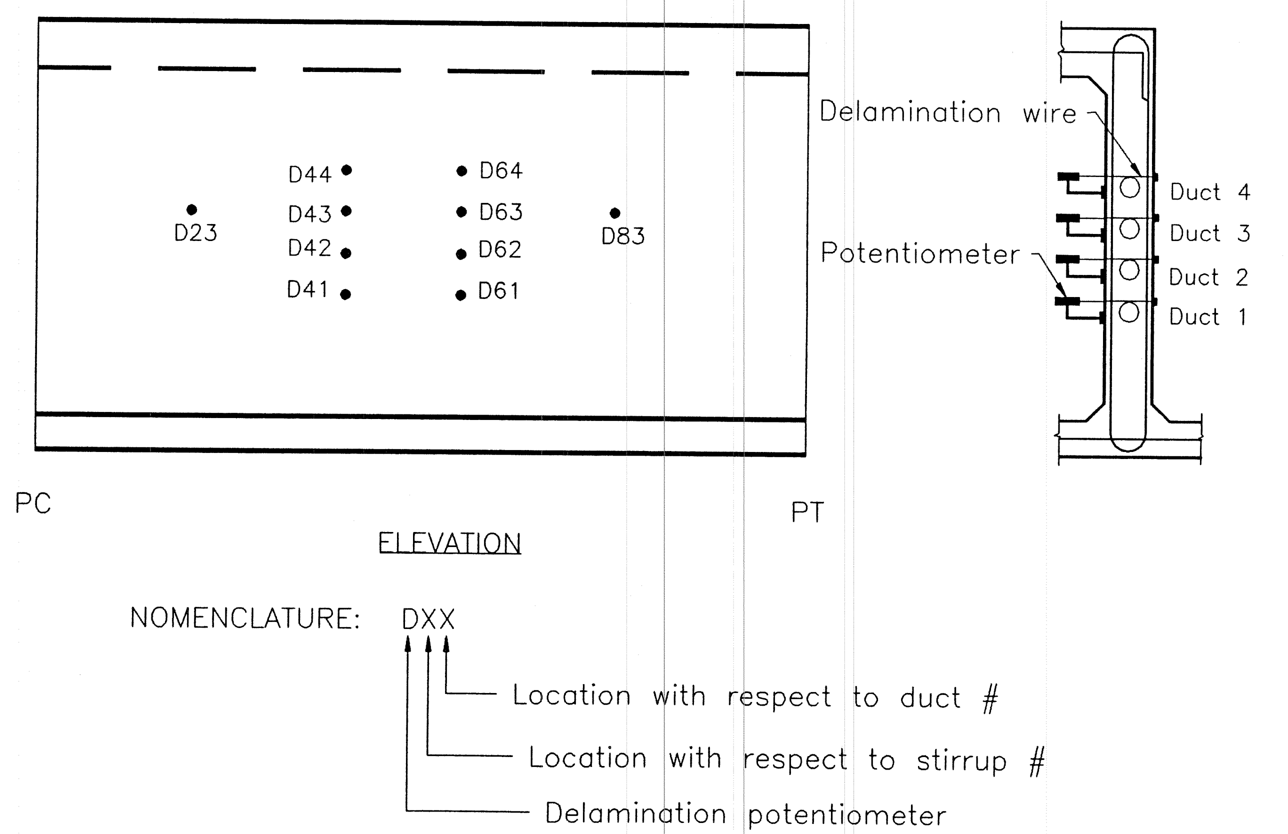

Figure 4.8 Delamination Gage Nomenclature

after it had been scanned.

4.3 Test Procedure

4.3.1 Ram-Pressure Transducer Calibration: Calibration of each of the 100 ton capacity hydraulic rams was performed in conjunction with the pressure transducer, pressure gage, switch and balance unit, and the pump which were later used for testing. All the hydraulic lines to be used were pressure tested to see whether they could sustain a pressure of 10,000 psi before being used. The purpose of the calibration was to obtain a relationship between the ram pressure and the microstrains indicated by the switch and balance. The calibrations were performed on a 600 kip SATEC Universal Testing Machine. The microstrain - ram pressure relationship is shown in Figure 4.9. The slope of the straight line was determined and was found to be the same for both the rams(Figure 4.9).

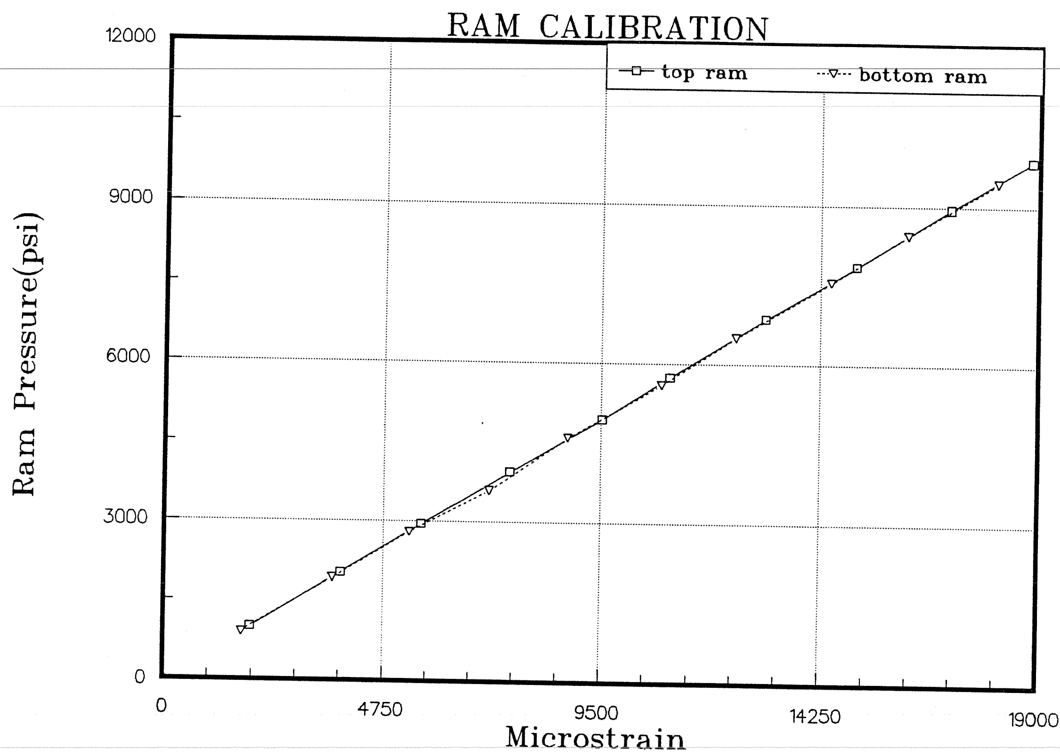

Figure 4.9 Ram Calibration

The calibration curve was used to control the force applied on the specimen during load application. A given jacking force was divided by twice the ram area(both rams have equal area) and corresponding to this value of ram pressure the value of microstrain was obtained. The switch and balance unit was then set to the above value of microstrain. The ram was then pumped until the needle in the switch and balance unit came to the zero position. The accurate pressure reading was obtained from the pressure transducer. The ram area(21.2 sq. inches for each ram), output rating and capacity of the pressure transducer were entered in the HPDAS program in the computer. The program calculated the exact jacking force and the switch and balance unit reading was just an analog system to control the approximate range of a predetermined load/pressure value.

4.3.2 Stressing Operation: In order to seat the tendons, each tendon was initially stressed to a pressure of 500 - 800 psi. All tendons in web DC were initially stressed to 500 psi. It was then observed that some of the tendons slackened as other tendons were being stressed. These strands were then stressed by adding 300 psi. Since the initial seating force in each strand was quite low, the difference in the load in each strand would not affect the test. In the case of web BC, the first strands stressed were stressed to 800 psi. The applied pressure was reduced to 500 psi for the strands stressed last. The steps involved in this operation are:

1) The loading frame, the rams and the bearing plate were aligned in a straight line and square to the web at the live end. On the dead end(north end) of the specimen, the reaction frame and the bearing plates were aligned in a straight line and square to the web ends.

2) The strand was threaded through the holes drilled in the loading frame into the ducts and out of the reaction frame on the north end of the specimen.

3) The wedges were then slipped on the strands and the chucks were positioned in place on both the live and the dead end.

4) The monostrand ram was then placed over the strand to be stressed at the live end. The monostrand rams were suspended from a cantilever bar welded to the loading frame. The monostrand was moved up or down with a winch from which it was suspended(Figures 4.10 & 4.11).

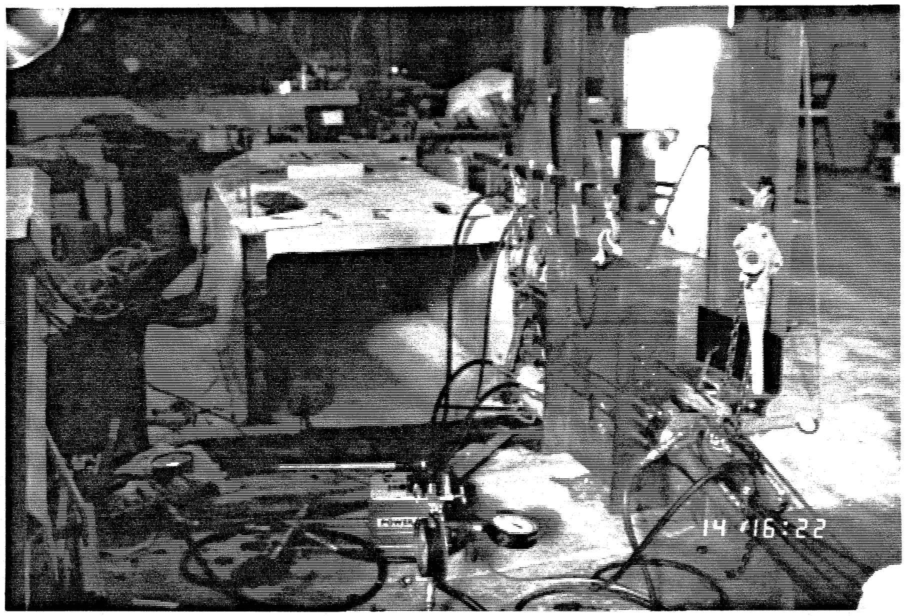

Figure 4.10 Monostrand Ram Suspended from a Winch

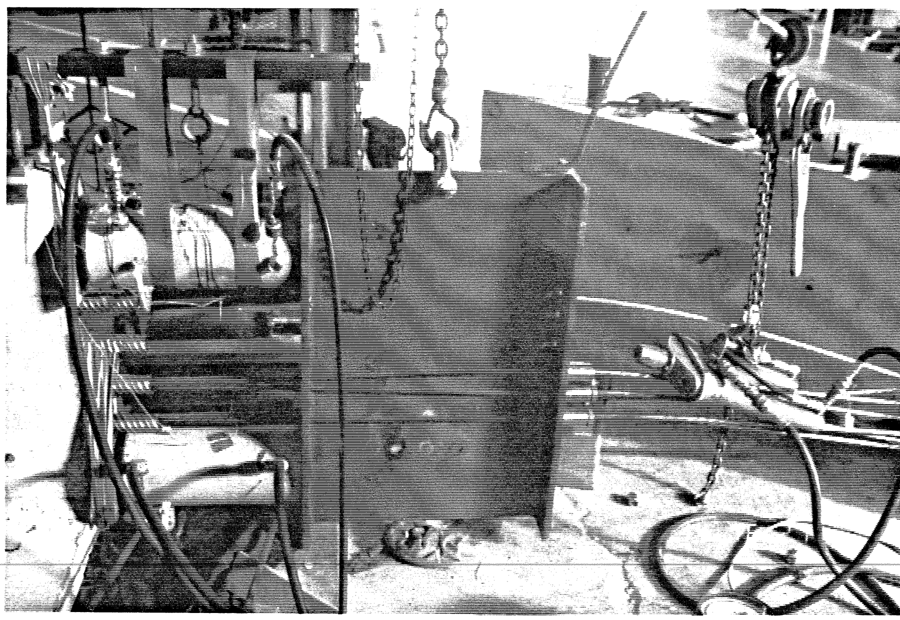

Figure 4.11 Monostrand Ram Suspended from a Winch

5) The ram was activated to a pressure in the range of 500 - 800 psi, stressing the individual strand.

6) While the above pressure was maintained the wedges were seated by applying a seating pressure of 1000 psi. A secondary pump was used to apply the seating pressure to the ram.

7) The seating pressure as well as the pressure in the tendons was released, and stressing equipment detached from the tendon.

8) The above procedure was repeated for all tendons. The stressing operation proceeded from the bottom-most to the top-most tendon.

4.3.3 Loading: Loading of the specimen began after all the strands had been seated. All the strands were stressed together during the loading operation by activating both the rams. Microstrain readings corresponding to the desired load increment were set on the switch and balance unit. Equal pressure was applied to both the rams so that the loading frame advanced equally in the horizontal direction from the web ends. A plot of jacking load and web deflection(in the case of web DC) or web delamination(in the case of web BC) was maintained to physically monitor the response at each load stage. At the end of each load stage, the data acquisition system was activated to read all channels of instrumentation as the test progressed. The strands were stressed until ultimate capacity of the web was reached. After failure of the specimen the ram pressure was released to end the test.

Chapter 5
TEST RESULTS

5.1 Introduction

Information obtained from instrumentation devices during the tests was analyzed and plotted as presented in the following sections. The jacking force for each web(DC & BC) is adjusted for the friction loss occurring in the tendons in order to reflect effective force at mid span of the specimen. The friction loss between the web ends and the center of the curve was found to be two percent of the load. Radial load(load acting in the radial direction of the web, F_r) in the web was determined by dividing the load at the center of the curve by the radius of curvature of the web. The stress in the stirrups was obtained by multiplying the strains measured by the strain gages by the elastic modulus of mild steel.

It was observed that web DC had an ultimate radial load capacity of 16.8 kips/ft., while the web BC withstood an ultimate radial load of 7.4 kip/ft. The first flexural cracking occurred approximately at a radial load of 3 kips/ft. in the web DC and at a radial load of 2.9 kips/ft. in the web BC, as shown in Figure 5.1.

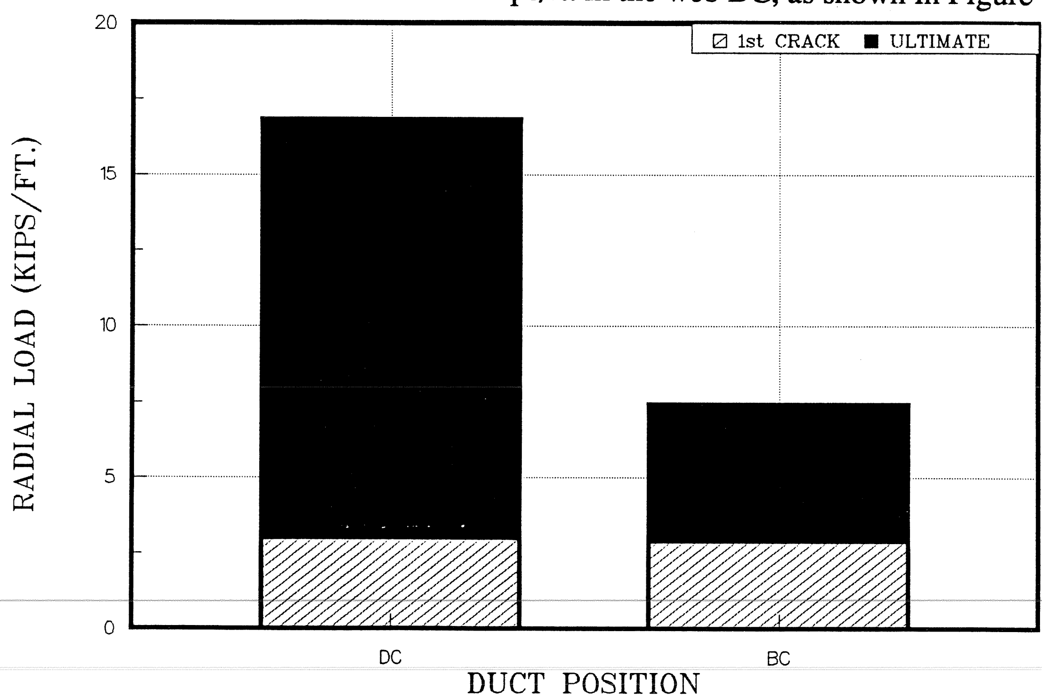

Figure 5.1 Specimen Capacities

5.2 Web Behavior

5.2.1 Behavior of Web DC: Figure 5.2 is a plot of radial load versus mid height web deflections. The mid height web deflections as measured at stirrup#4 and #6 were equal throughout the load history of the web. All the mid height deflections measured follow the same pattern. The deflections measured near the straight section(WS2 and WS8) were less as compared to the deflections measured in the center region(WS4 and WS6) of the web. The mid height web deflections increased linearly with an increase in the radial load until the web was loaded to a radial load of 3 kips/ft. As the radial load was further increased, the mid height deflections increased linearly but the slope of the response was reduced. The stirrup stresses also increased linearly with an increase in radial load(Figures 5.3 and 5.4). A reduction in the slope of the linear relation between mid height stirrup stress(IM) and radial load occurred beyond the radial load of 3 kips/ft. as seen in Figure 5.3. This indicates that flexural cracking of the web probably occurred at a radial load of 3 kips/ft. at the mid height of the web. The first crack was visually observed at a radial load of 10.26 kips/ft.

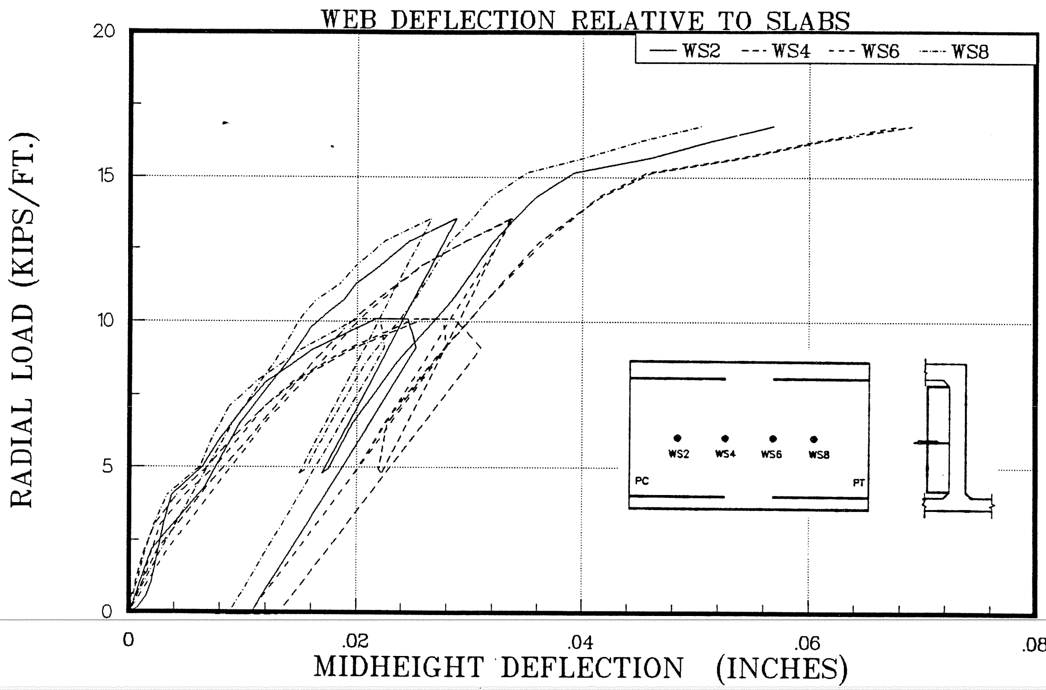

Figure 5.2 Mid Height Web Deflections of Web DC

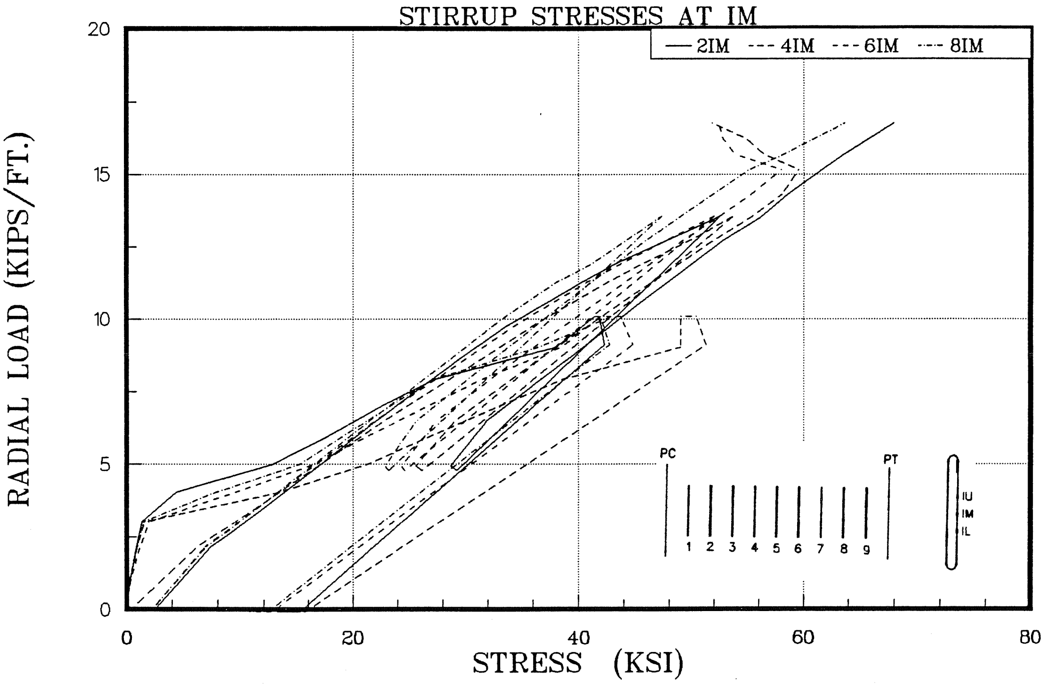

Figure 5.3 Mid Height Stirrup Stresses of Web DC

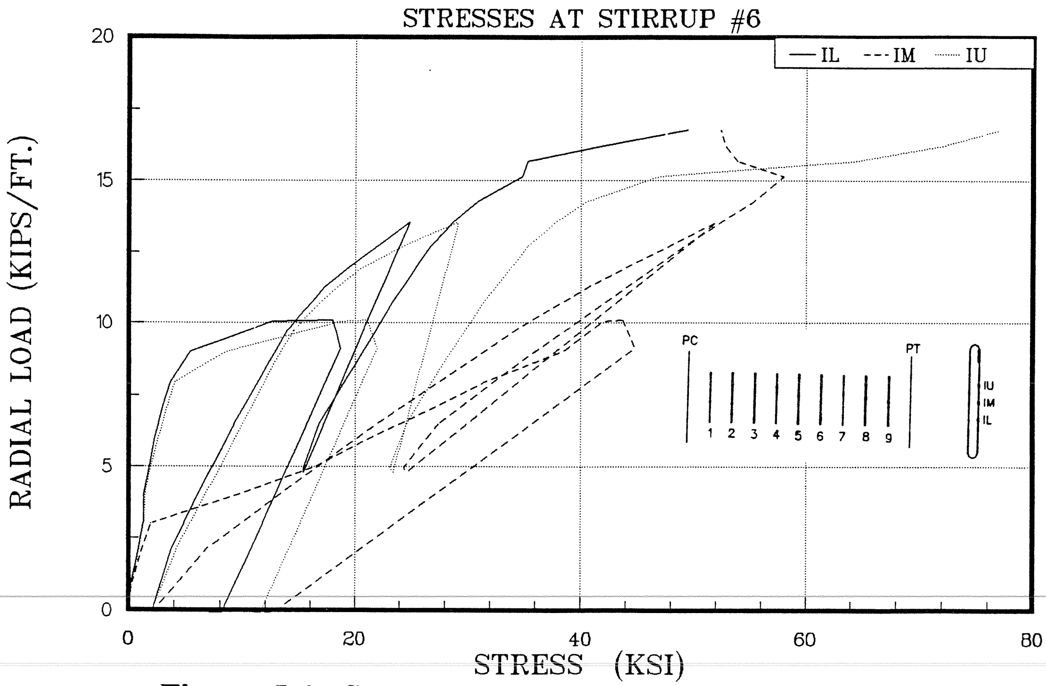

Figure 5.4 Stresses at Stirrup #6 of Web DC

Precaution was taken not to go near the web due to safety reasons. A theodolite and an automatic level were used to observe and detect cracks from a distance. As observed in Figure 5.4 there was a sharp increase in stresses at the IU and IL strain gage locations at a radial load level of 8 kips/ft. and 9.2 kips/ft. This probably indicated flexural cracking of concrete at these locations. The relationship between the stirrup stresses remained linear beyond the respective cracking loads.

Delamination of the inside face of the web started at a radial load of 15.2 kips/ft. as shown in Figures 5.5 and 5.6. The web then failed explosively at a radial load of 16.82 kips/ft. without any visual or audible warning. The web concrete spalled off and travelled as far as 35 ft. from the web(Figure 5.7). The mid height web deflection and the IU and IL stresses increased linearly with an increase in radial load between 15.2 kips/ft. and 16.82 kips/ft. It was observed that there was a sharp increase in the mid height deflections and the IL and IU stirrup stresses in this load range. The mid stirrup stresses(IM) for stirrup #4 and #6 underwent a load reversal(decrease in stress with an increase in radial load). This phenomenon suggests formation of a mechanism(Figure 5.8) at the mid height of the inside face

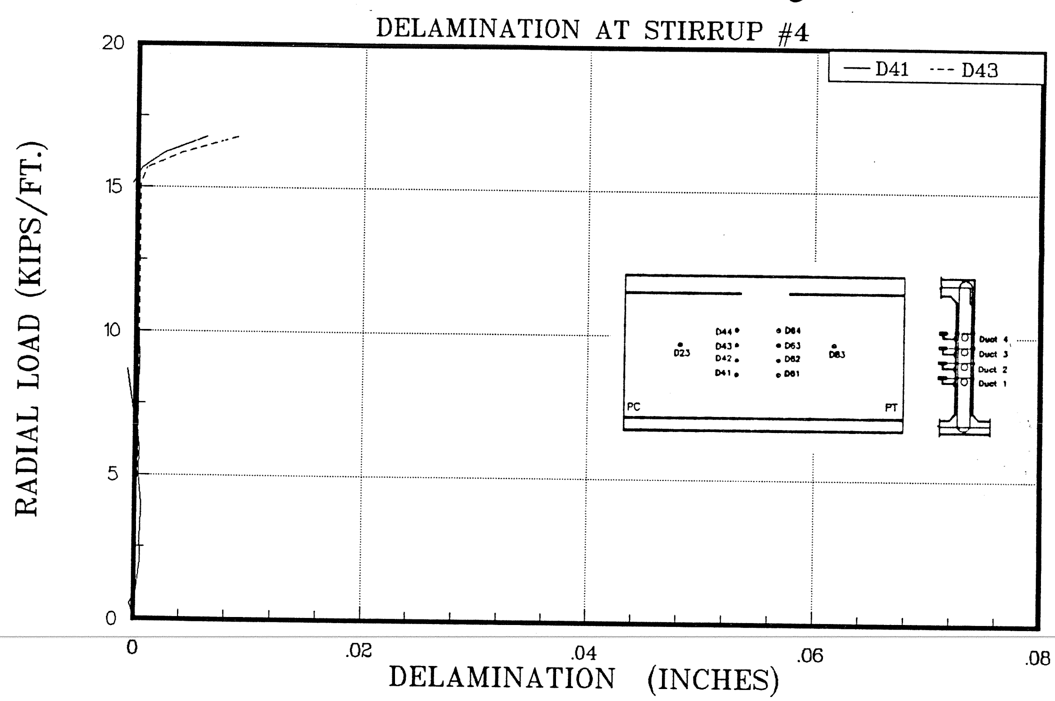

Figure 5.5 Delamination at Stirrup #4 of Web DC

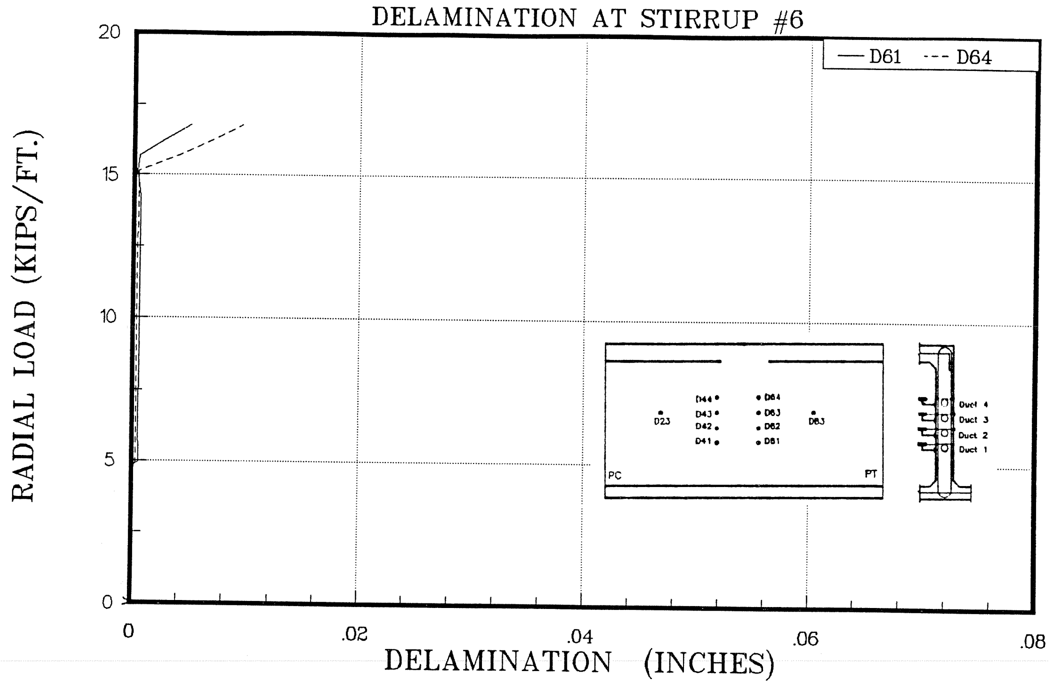

Figure 5.6 Delamination at Stirrup #6 of Web DC

of the web and redistribution of forces. The maximum IM stresses(stress at 4IM = 59.2 ksi) were much below the stirrup yield strength(75 ksi) at the load stage of 15.2 kips/ft., so the bars did not yield at the mid height of the web.

Delamination just above the bottom duct was observed at a radial load of 15.7 kips/ft. The IU stresses were 30% higher than that of IL stresses at the radial load stage of 15.2 kips/ft. and about 60% higher at the failure load of 16.82 kips/ft. The web delamination started just above the top and the bottom duct suggesting a shear failure at these locations. The shape of the crack observed suggests a diagonal tension failure at the IU and IL levels. At the radial load of 15.2 kips/ft. these cracks propagated diagonally and finally became vertical and parallel to the web face(Figure 5.9) just behind the ducts. This crack formation allowed all four ducts to breakout from the web. Figures 5.10 & 5.11 show the web immediately after failure. Breakout of the ducts caused the stirrups to pullout from the lap joint near the top slab(Figure 5.12). Web delamination at the mid height of

Figure 5.7 Concrete Fragments in Front of the Web

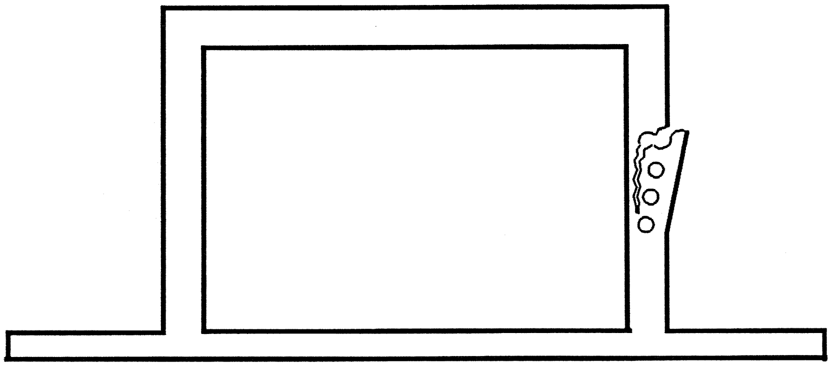

Figure 5.8 Mechanism at Radial Load 15.2 kips/ft.

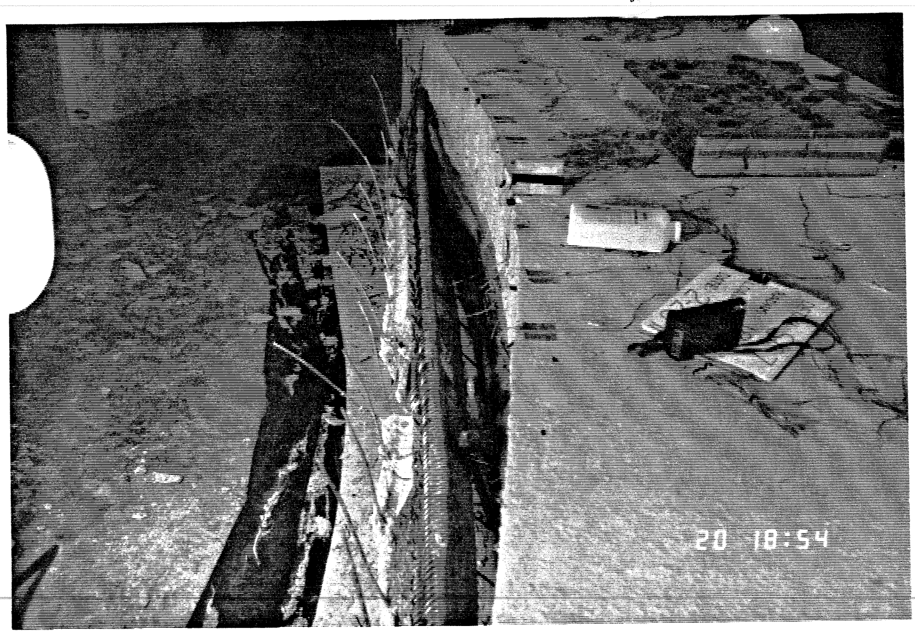

Figure 5.9 Web DC at Failure

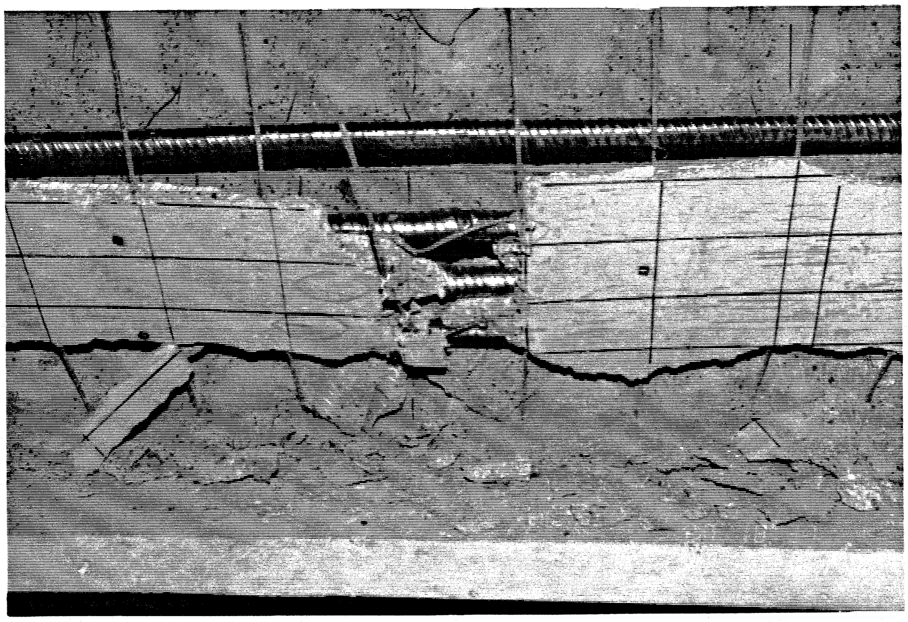

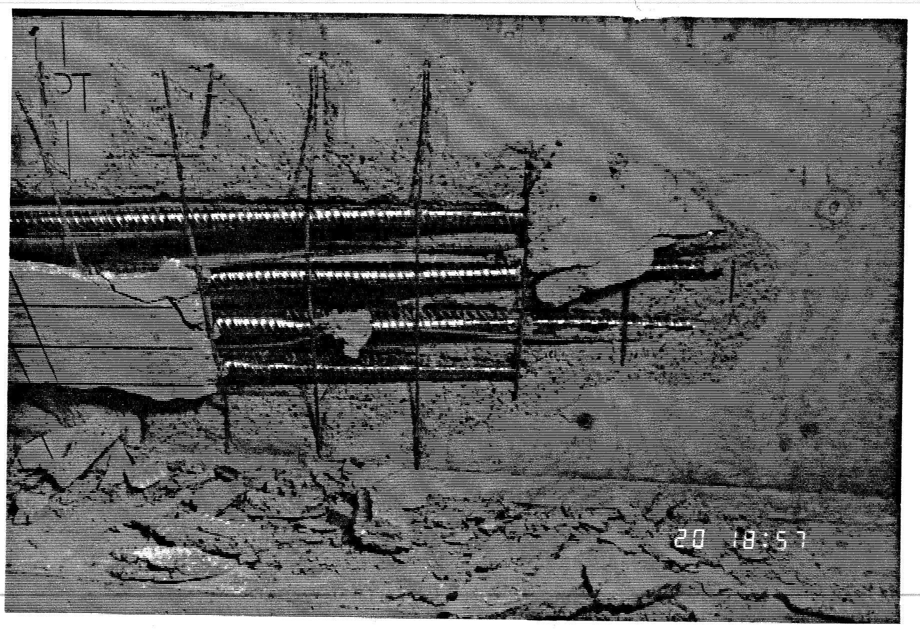

Figure 5.10 Web DC at Failure

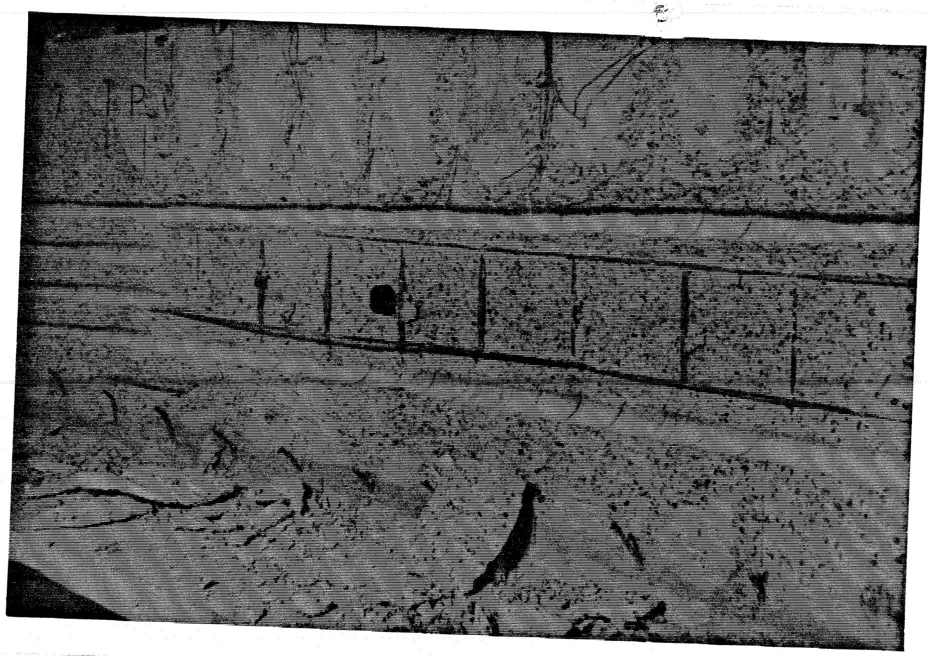

Figure 5.11 Crack Pattern Behind the Ducts

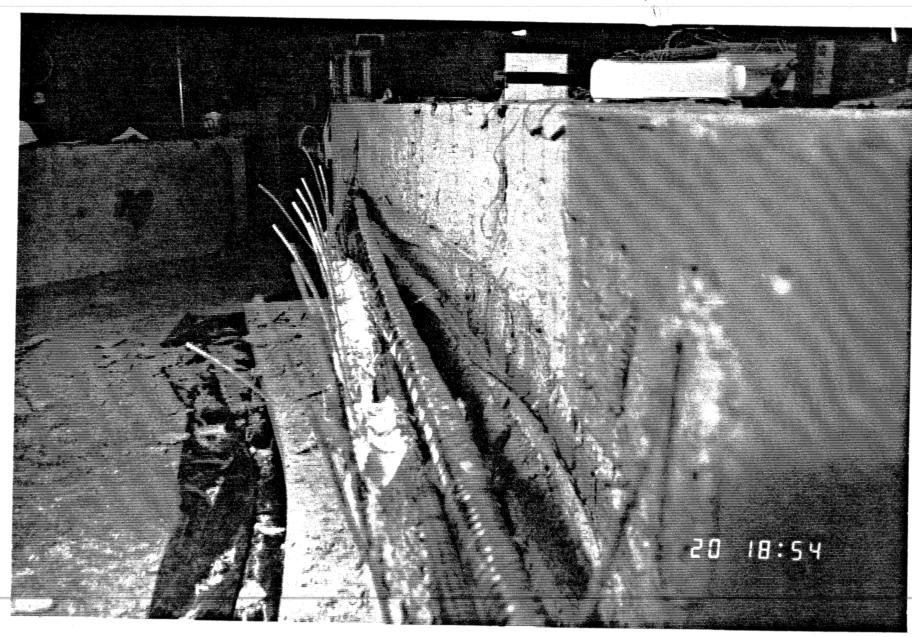

Figure 5.12 Pullout of Stirrups

the web(center line of the duct arrangement) was less compared to the delamination just above the top duct and just below the bottom duct. This indicates that the concrete cover over the duct on the inside face did not act as a local beam.

5.2.2 Behavior of Web BC;: Figure 5.13 shows a plot of mid-height deflections measured relative to the bottom and top slabs versus radial load acting on the web. Figure 5.14 is a plot of the web mid-height deflections in the curved section relative to the web deflections at PC and PT versus the radial load. These graphs show a multi linear relationship between the mid-height deflections and radial load. At a radial load level of 2.9 kips/ft.(1.9 kips/ft. for WS6), a marked decrease in the slope of the line is observed as shown in Figures 5.13 & 5.14. This sudden increase in the mid-height deflections suggests the flexural cracking of concrete on the inside face of the web at its mid-height. Figure 5.15 shows the variation of mid-height stirrup stresses(IM) on the inside face of the web. This graph shows a linear increase of IM stresses with an increase in radial load until a radial load level of 2.9 kips/ft. Beyond the radial load level of 2.9 kips/ft. the IM stresses still show a linear relation with lateral loads but with a reduced slope. It is

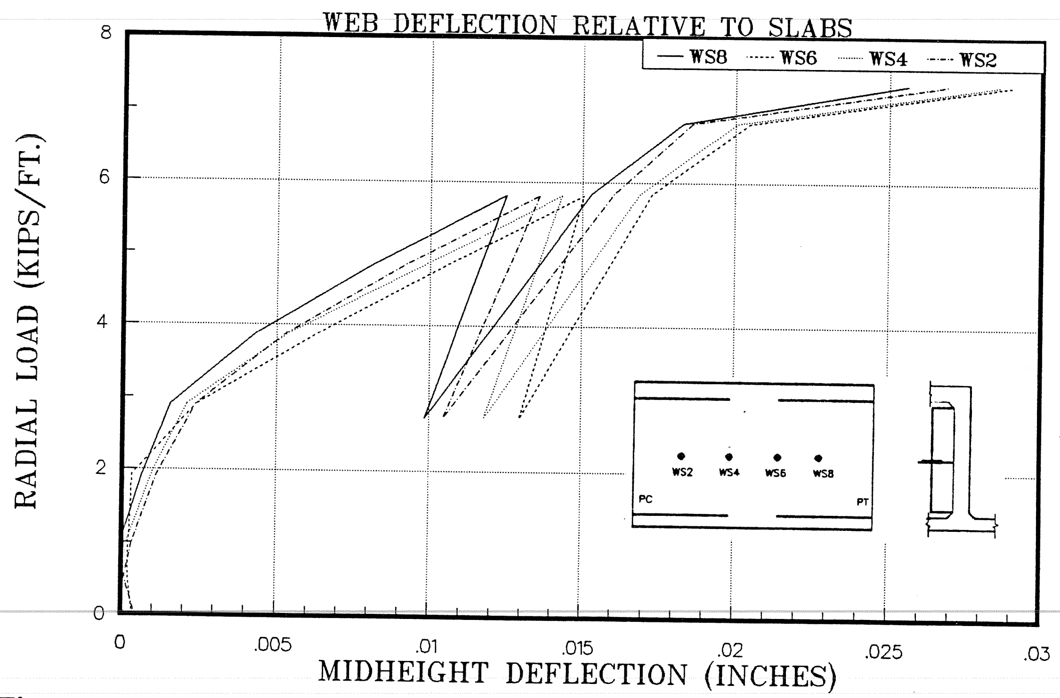

Figure 5.13 Mid-Height Web Deflections Relative to Slab of Web BC

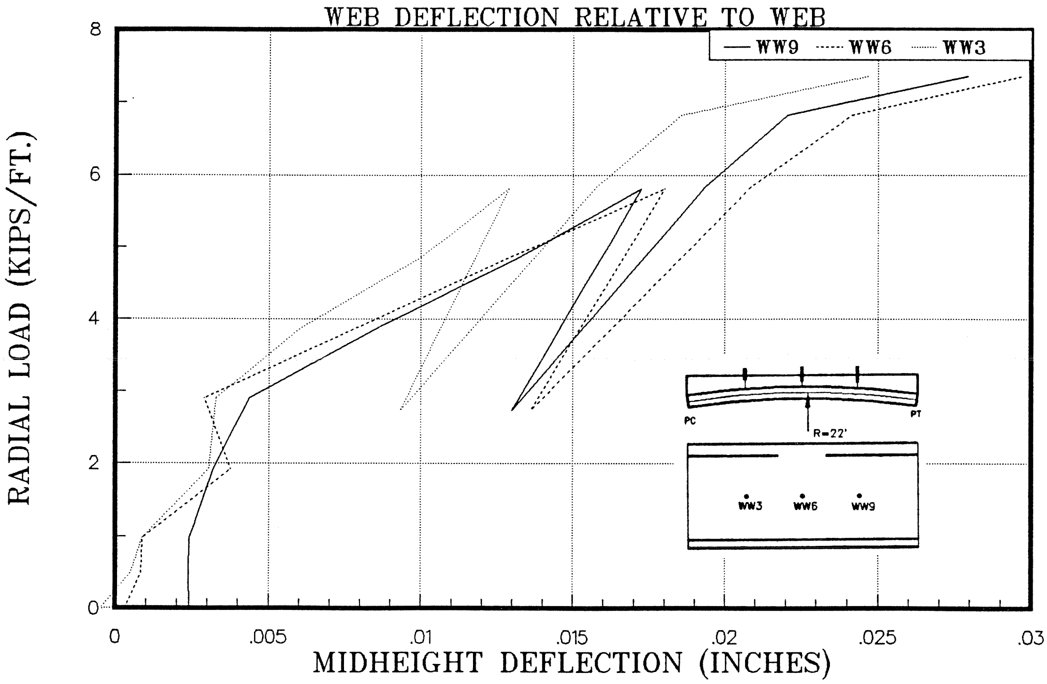

Figure 5.14 Mid Height Web Deflections Relative to Web at PC & PT of Web BC

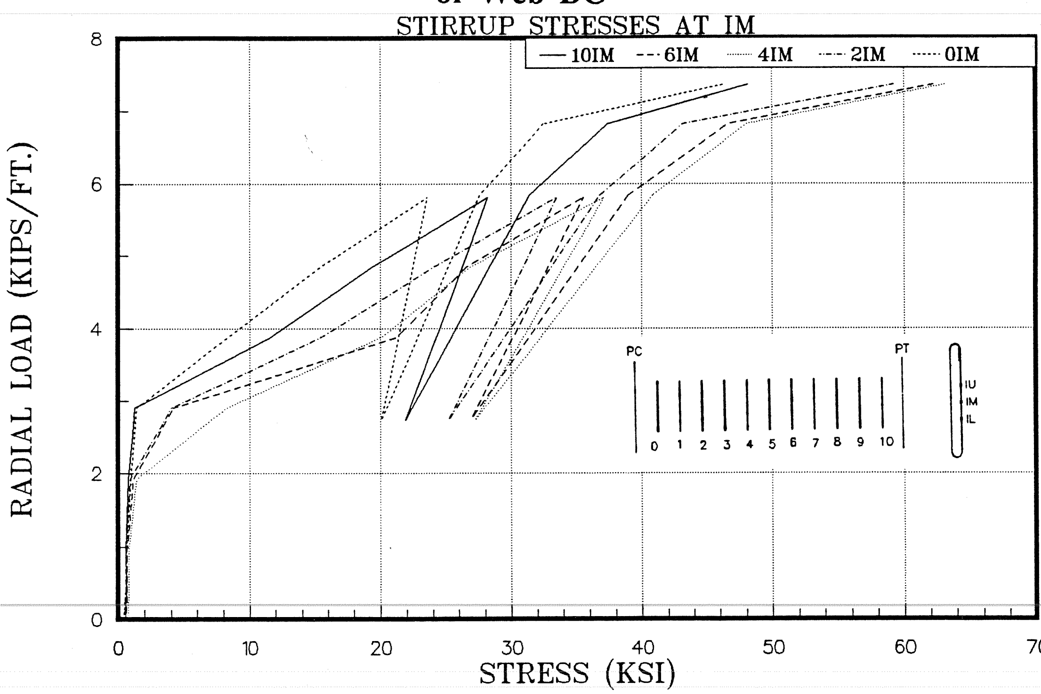

Figure 5.15 Mid Height Stirrup Stresses of Web BC

observed that the IM stirrup stresses at stirrups #2, #4 and #6(central portion of the curve) show the reduction in slope at a radial load of 1.9 kips/ft. This observation suggests that the flexure cracks initiated in the central part of the curve at mid-height and were followed by flexural cracks all along the mid height of the curve at a radial load of 2.9 kips/ft. The first cracks were visually observed at a radial load of 4.85 kips/ft. using a theodolite as an optical remote sensing device.

Figures 5.16 & 5.17 show the relationship between stirrup stresses at the IL, IM and IU levels for stirrup #4 and #6 with the radial load in the web. The stirrup stresses increased linearly with an increase in radial load. A reduction in the slope of the line occurs for the IU stresses beyond the radial load of 3.87 kips/ft. for both stirrup #4 and #6(Figures 5.16 &5.17). This suggests cracking of concrete at or near the IU gages. A sharp increase in stirrup stresses was also observed at both IU and IL levels beyond the radial load of 4.85 kips/ft. This suggests concrete cracking at or near these locations. The stirrup stresses at IL, IM, IU locations increased linearly from these cracking lateral loads to a load level of 6.83 kips/ft. The mid height deflections also increased linearly between the radial

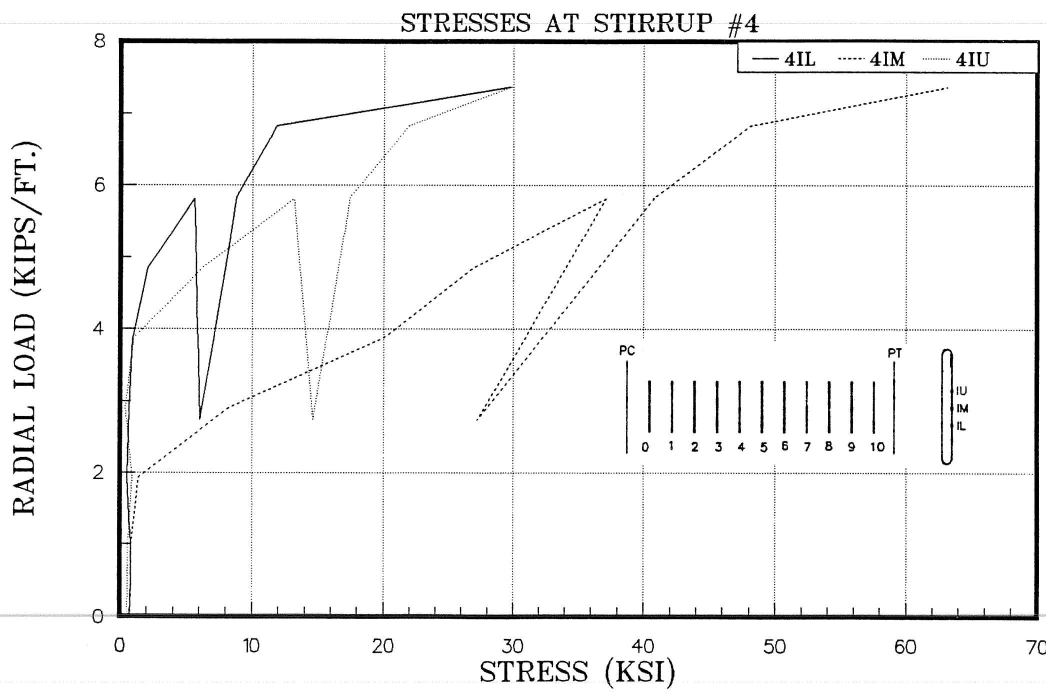

Figure 5.16 Stresses at Stirrup #4 of Web BC

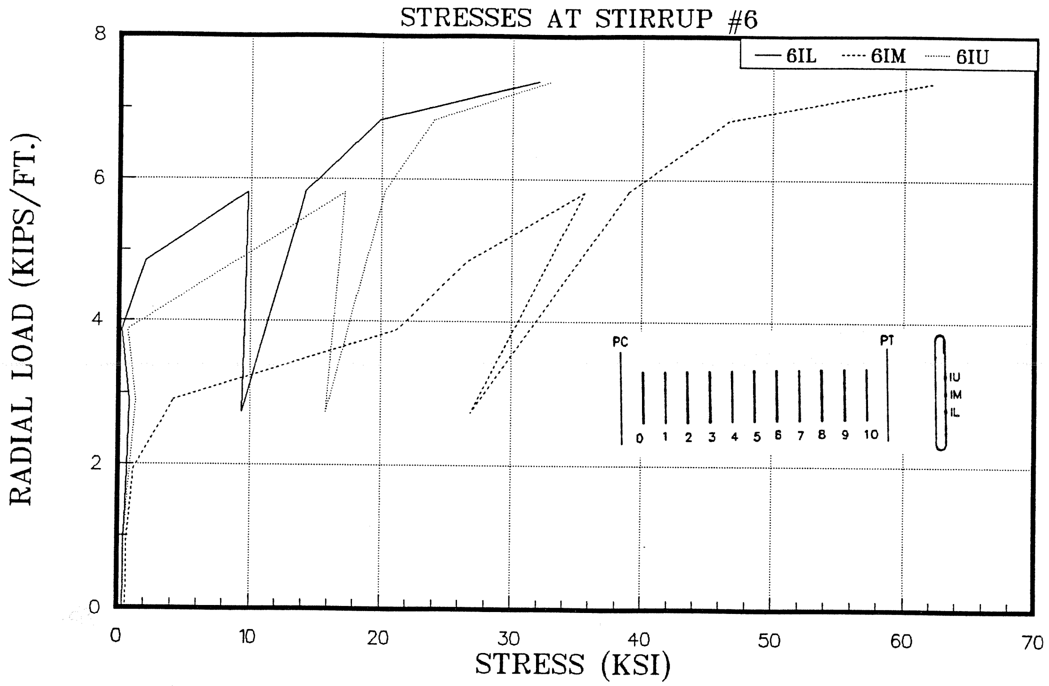

Figure 5.17 Stresses at Stirrup #6 of Web BC

load of 2.9 kips/ft. and 6.83 kips/ft.(Figures 5.13 & 5.14). Between a radial load level of 6.83 kips/ft. and the next radial load level of 7.36 kips/ft.(failure load) the stirrup stresses increased steeply. Mid-height deflections also register a sharp increase in this load interval. At 7.36 kips/ft. the web stopped taking any more load and the web cover on the inside face of the web moved away from the rest of the web.

Marked increases in delamination above the ducts at stirrups #4 and #6 with an increase in radial load in the web are shown in Figures 5.18 and 5.19. It was observed that the delamination started and was greatest at the center line of the duct arrangement(D42 & D62, henceforth referred to as DX2). Delamination at DX2 started to occur at a radial load of 2.9 kips/ft. D43 and D63 started delaminating shortly thereafter. DX1 gages which were symmetrical to the DX3 gages about the center line of the tendon group began to register delamination at a radial load of 4.0 kips/ft. and lagged much behind the DX3 gages. It was observed that the delamination was greatest at the center of the duct arrangement and no

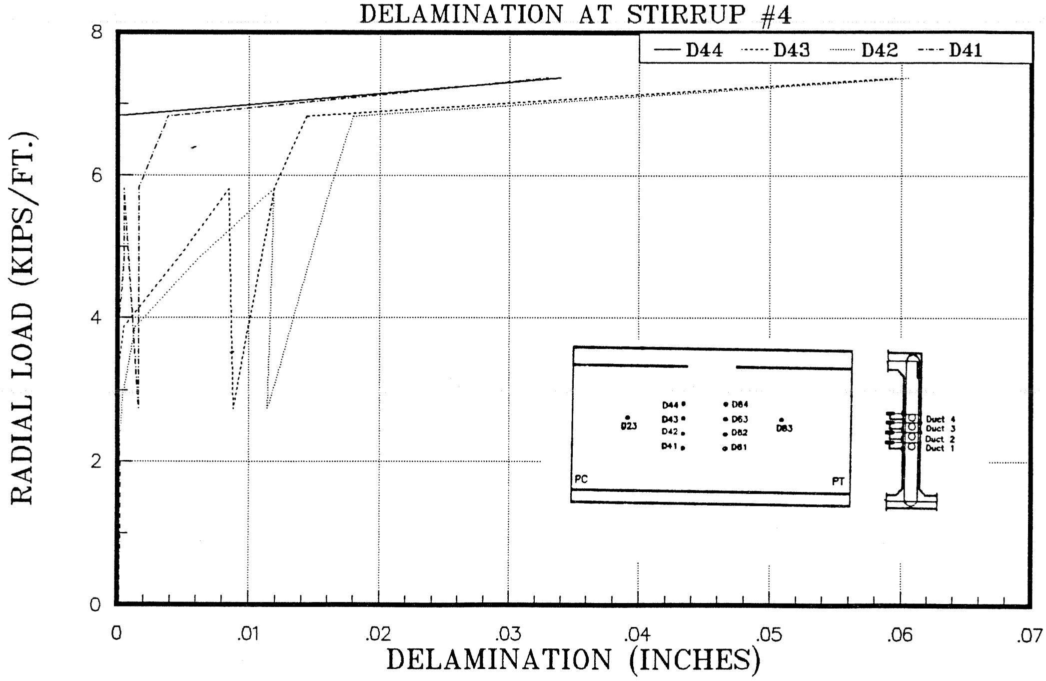

Figure 5.18 Delamination at Stirrup #4 of Web BC

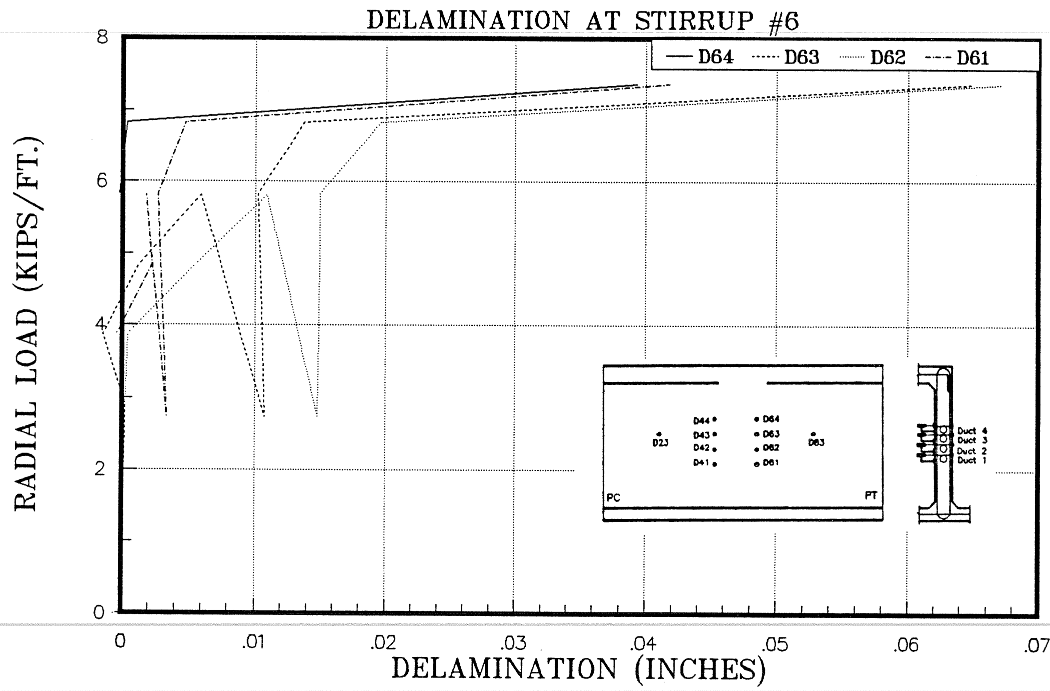

Figure 5.19 Delamination at Stirrup #6 of Web BC

delaminations was registered at the top of the tendon group until large scale cracking was observed. This suggests high flexural deflections in the cover over the ducts between the top and bottom duct. The duct cover between the top and bottom slab acted like a local beam. Delamination at DX1 and DX4 were equal between the radial load level of 6.83 kips/ft. and 7.36 kips/ft.(failure load).

The failure in the web occurred due to diagonal tension failure of concrete. The crack started near the top and bottom ducts probably near the last flexural crack in the local beam(spanning from the top of the top duct to the bottom of the lower most duct) at the load level of 6.83 kips/ft. The crack propagated out and up and out and down as shown in Figures 5.20 & 5.21. A non explosive failure occurred at the next load level of 7.4 kips/ft. The failure took place with some visual and audible warning as shown in Figures 5.22 - 5.26.

Figure 5.20 Crack Pattern of Web BC

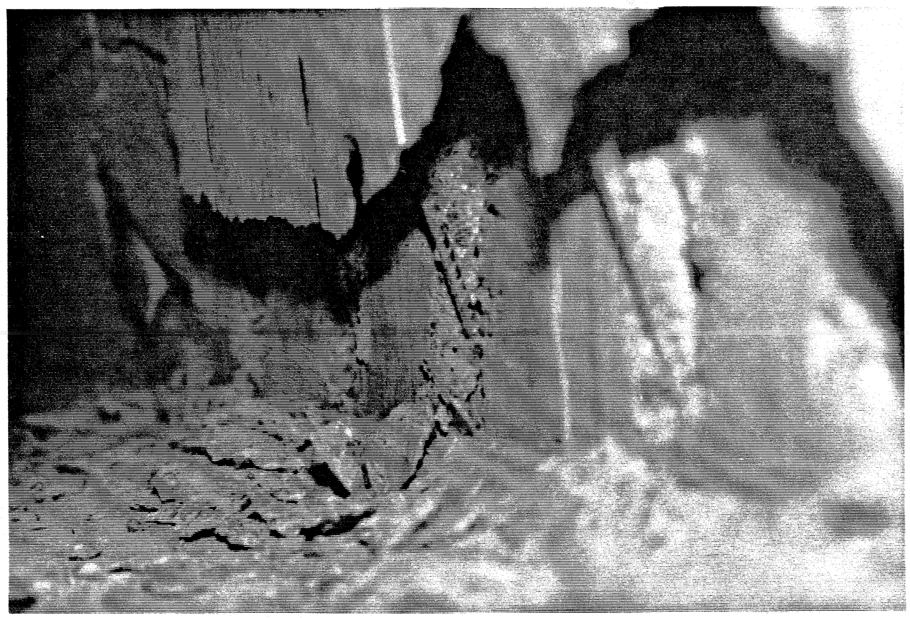

Figure 5.21 Crack Pattern of Web BC

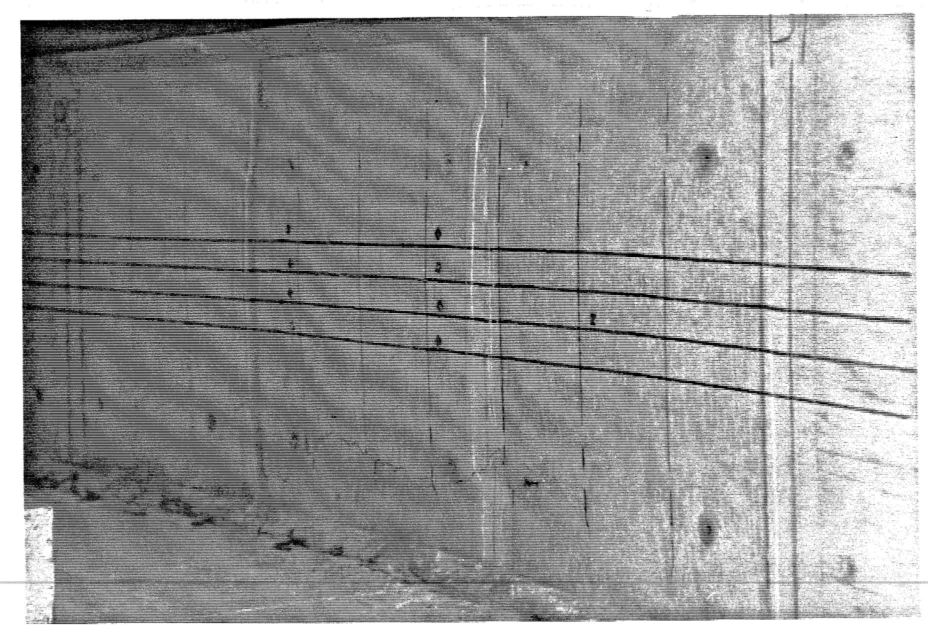

Figure 5.22 Web BC Just Before Failure

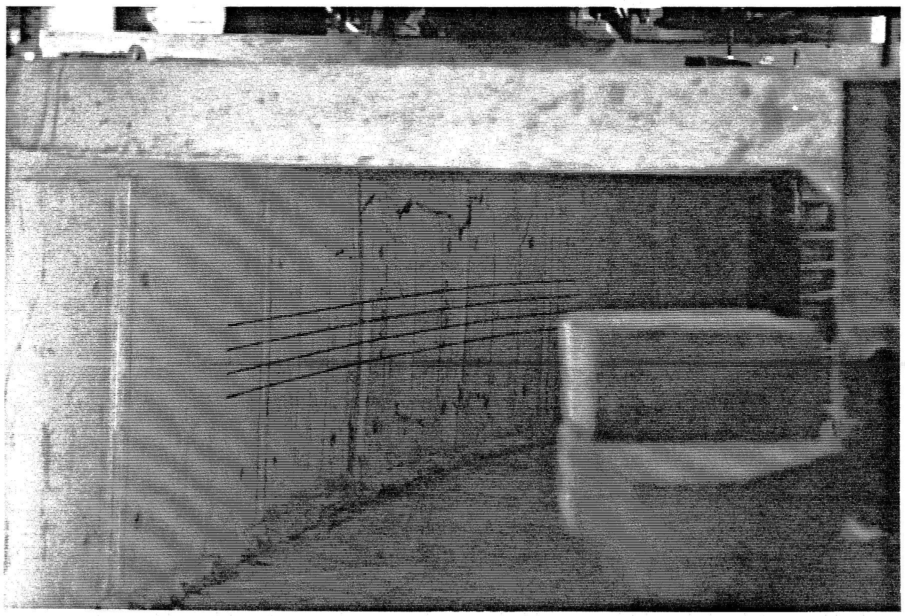

Figure 5.23 Web BC at Failure

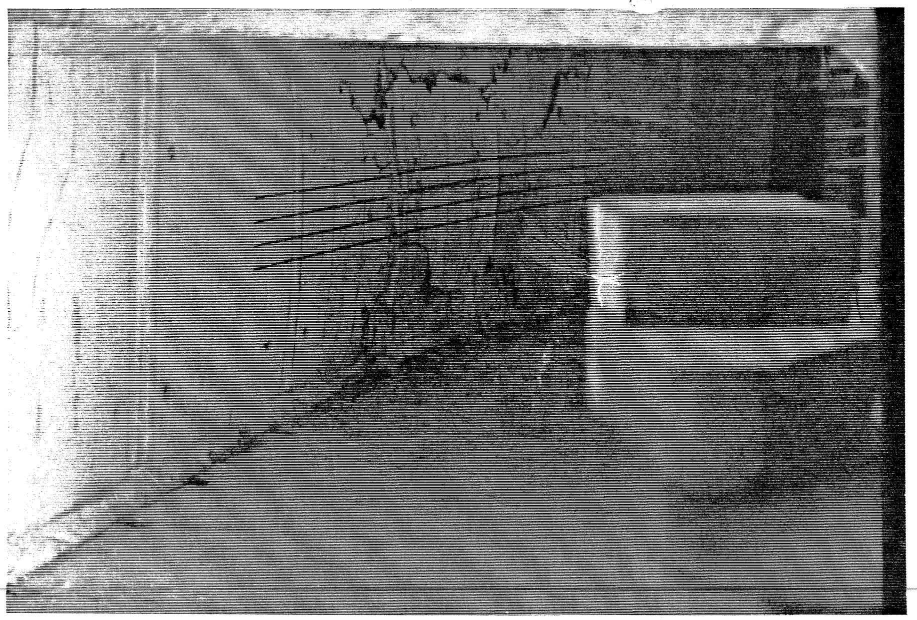

Figure 5.24 Web BC after Failure

Figure 5.25 Web BC after Failure

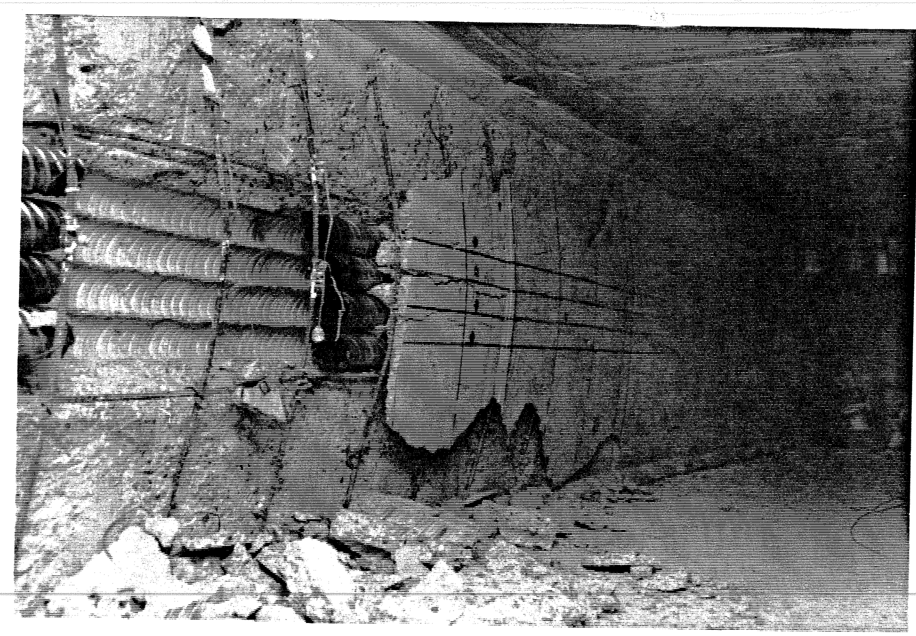

Figure 5.26 Web BC after Cutting the Ducts

5.2.3 Comparison of Behavior of Web BC and DC: Web DC had a higher capacity to resist breakout forces imposed post-tensioning of the tendons when compared to the web BC(Figure 5.1). Web DC sustained a radial load of 16.82 kips/ft. while web BC was able to resist a maximum radial load of only 7.4 kips/ft. Web DC failed explosively without any visual or audible warning, preceded only by small longitudinal cracks at the tendon level. The failure of web BC was not explosive like that of the web DC and was preceded by large longitudinal cracks at the tendon level and about a foot above and below the center line of the duct arrangement(Figure 5.22). Both of the webs failed due to tensile splitting of concrete caused by high shear developed in the web from the radial load(Figures 5.25 & 5.26). In the case of web BC the duct cover on the inside face of the web acted like a local beam.

Both webs showed measurable and somewhat trilinear patterns between the mid height web deflections and the radial load(Figure 5.27). Stirrup

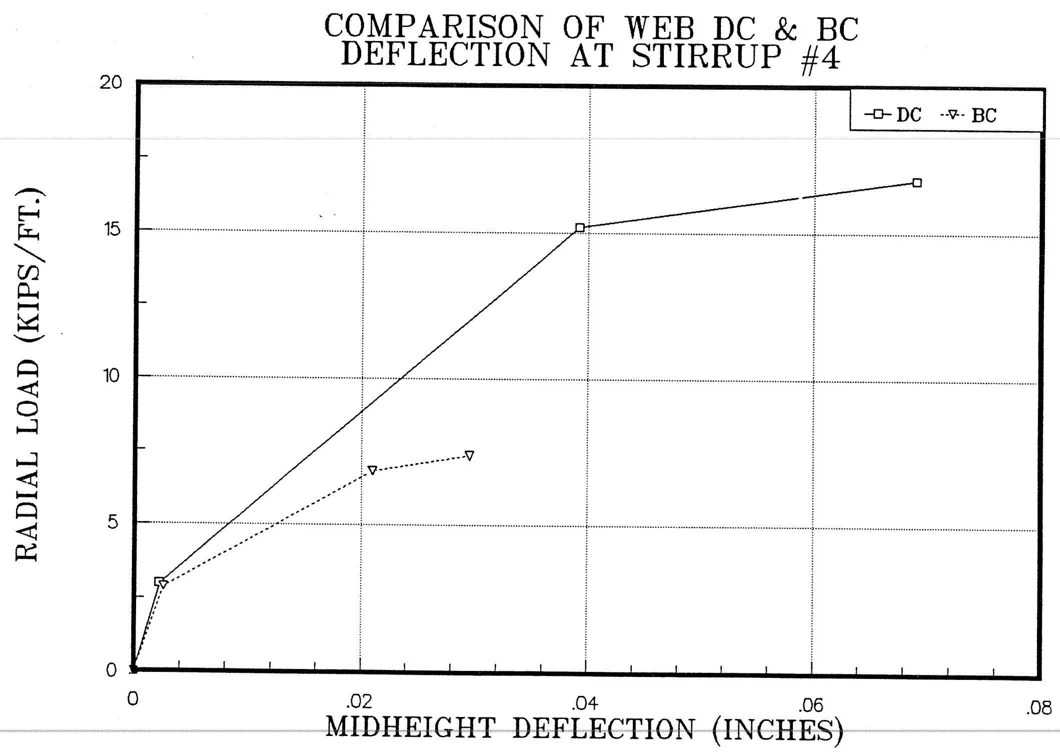

Figure 5.27 Similarity in Behavior of Web DC & BC

stresses also varied in a similar fashion with radial load in both the webs. Stirrup stresses showed an increase just after cracking in both of the webs. Increases in delamination was observed in both the webs just before failure. Large delaminations in web BC were observed at the mid height levels due to local beam action of the duct cover. Delamination was observed at a much lower radial load in the web BC as compared to the web DC. Increases in delamination of the web DC were observed just above the top duct and just below the bottom duct. The delamination in DC indicates a shear failure near the top and the bottom duct.

The flexural capacity of a web is calculated as shown in Figure 5.28. The web is assumed as a simply supported beam with simple supports at the connection with the slabs as suggested by CALTRANS. The moments thus obtained are reduced by 20 percent to consider continuity between the slabs and the web(Reference 3). As seen in Figure 5.28 the moment acting on the web which is calculated by this recommendation is greater than the ultimate flexural capacity of the web. From the strain gage data it can be seen that yielding of the stirrups does not occur. This is probably because the load is being transferred along the longitudinal direction of the curved beam. The curved portion of the beam acts like an arch. Significant portion of the load is probably carried by the arching action of the curved beam.

5.3 Design Indications

Failure in both of the webs occurred due to splitting of concrete in the web. The splitting failure planes for each of the webs are shown in Figures 5.29 & 5.30 respectively. Duct positioning affects the type of failure plane which may govern and is an important parameter in design.

The resistance of concrete to tendon breakout can be improved by proper duct positioning along the web cross-section in the curved portion of the girder. It is probable that by increasing the web thickness and hence the effective cover that there would be an increase in the resistance of the web to breakout forces.

Radial shear stress in the web can be expressed as $v = F_r/2bd_e$, where F_r, b and d_e are defined in Figure 5.31.

Moments on the Web at Failure Load (CALTRANS approach)

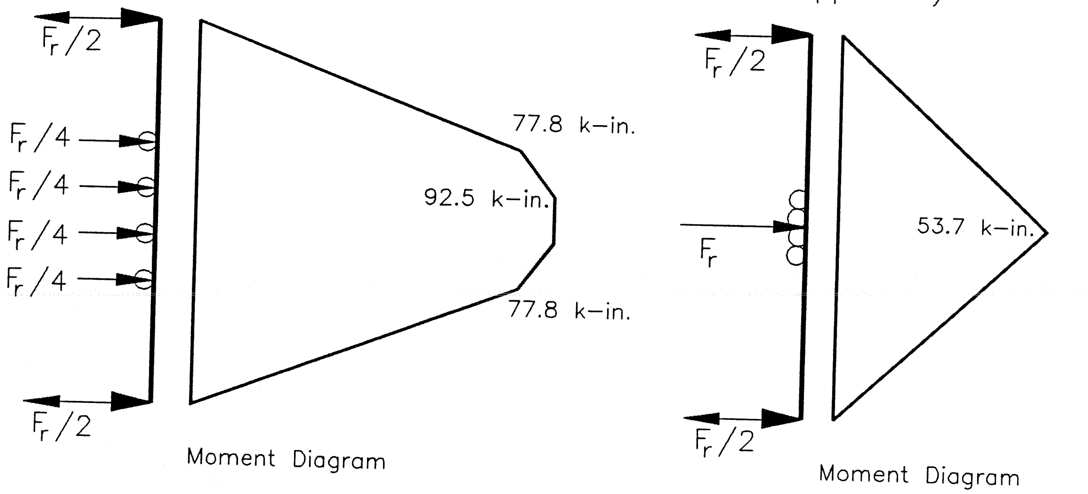

WEB – DC

$F_r = 16.82$ kips/ft.

$M_{max} = 92.5$ k-in.

$M_u = 0.8\ M_{max} = 74$ k-in.

WEB – BC

$F_r = 7.4$ kips/ft.

$M_{max} = 53.7$ k-in.

$M_u = 0.8\ M_{max} = 42.9$ k-in.

Ultimate Moment Capacity

For both the webs

$d = 3.26"\quad b = 12"$

$A_S = 0.044(12/7) = 0.075\ in^2$

$C = T$

$$a = \frac{0.075\ in^2\ (75\ ksi)}{(0.85x6ksi)(12")} = 0.092"$$

$$M_n = (0.075\ in^2)(75\ ksi)(3.26" - 0.092"/2) = 18.08\ k\text{-}in.$$

therefore $M_u \gg M_n$

Figure 5.28 Flexural Check of the Webs

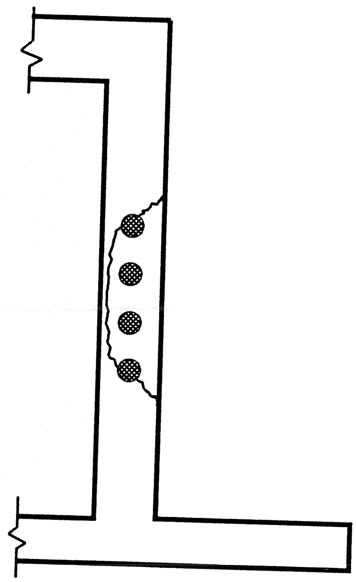

Figure 5.29 Splitting in Web DC at F_r=16.82 kips/ft.

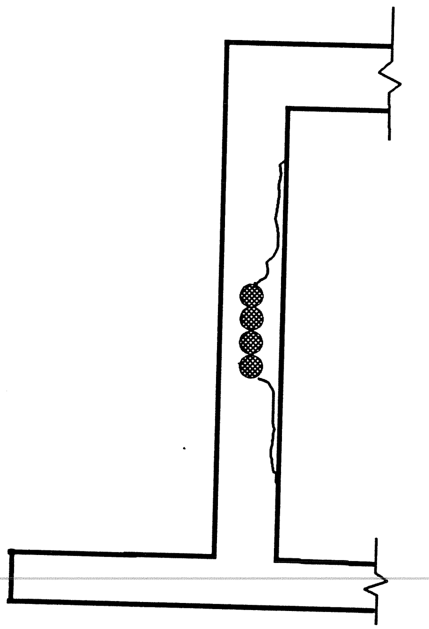

Figure 5.30 Splitting in Web BC at F_r=7.4 kips/ft.

Therefore, the radial shear stresses in the webs DC and BC at failure are

$v_{web\ DC}$ = 16.8 kips/ft./(12"x 2(4" - 1.75")) = 0.311ksi

$v_{web\ BC}$ = 7.4 kips/ft./(12"x 2(1.125")) = 0.274 ksi

$v/\sqrt{f_c'}$ = 311 psi /$\sqrt{5951}$ psi = 4.03 for web DC

$v/\sqrt{f_c'}$ = 274 psi /$\sqrt{5984}$ psi = 3.54 for web BC

Experimental studies(References 8,9 &10) on beams show that the ratio of shearing stress at failure to $\sqrt{f_c'}$ ($v/\sqrt{f_c'}$) varies between 2 and 4. As illustrated above the ratio of shear strength of concrete at failure to $\sqrt{f_c'}$in the webs BC and DC lies between 2 and 4. AASHTO and the ACI Building Code Requirements limit the concrete shear strength to $2\sqrt{f_c'}$ unless the ratio of shear to moment(V_u/M) at the critical section is checked. Based on the two tests it is recommended that designers use $2\sqrt{f_c'}$ as a conservative limit for the shear strength of concrete until further tests are performed. It should be required that the radial load on the web be less than or equal to the concrete shear strength($F_r \geq 2V_c$) as shown in Figure 5.31. The concrete shear strength in the expression defining V_c is prescribed as $2\sqrt{f_c'}$ as illustrated in Figure 5.31.

The shear failure model described in Figure 5.31 for bundled tendons and for ducts spaced at one duct clear spacing can be used to determine the radial shear capacity of the web. If the ducts are bundled in the web and if the radial shear stress exceeds $2\sqrt{f_c'}$ then the designer should increase the thickness of the web or provide one duct clear spacing between the ducts. If the ducts are positioned at one duct clear spacing and the radial shear stress exceeds $2\sqrt{f_c'}$ then the web thickness should be increased.

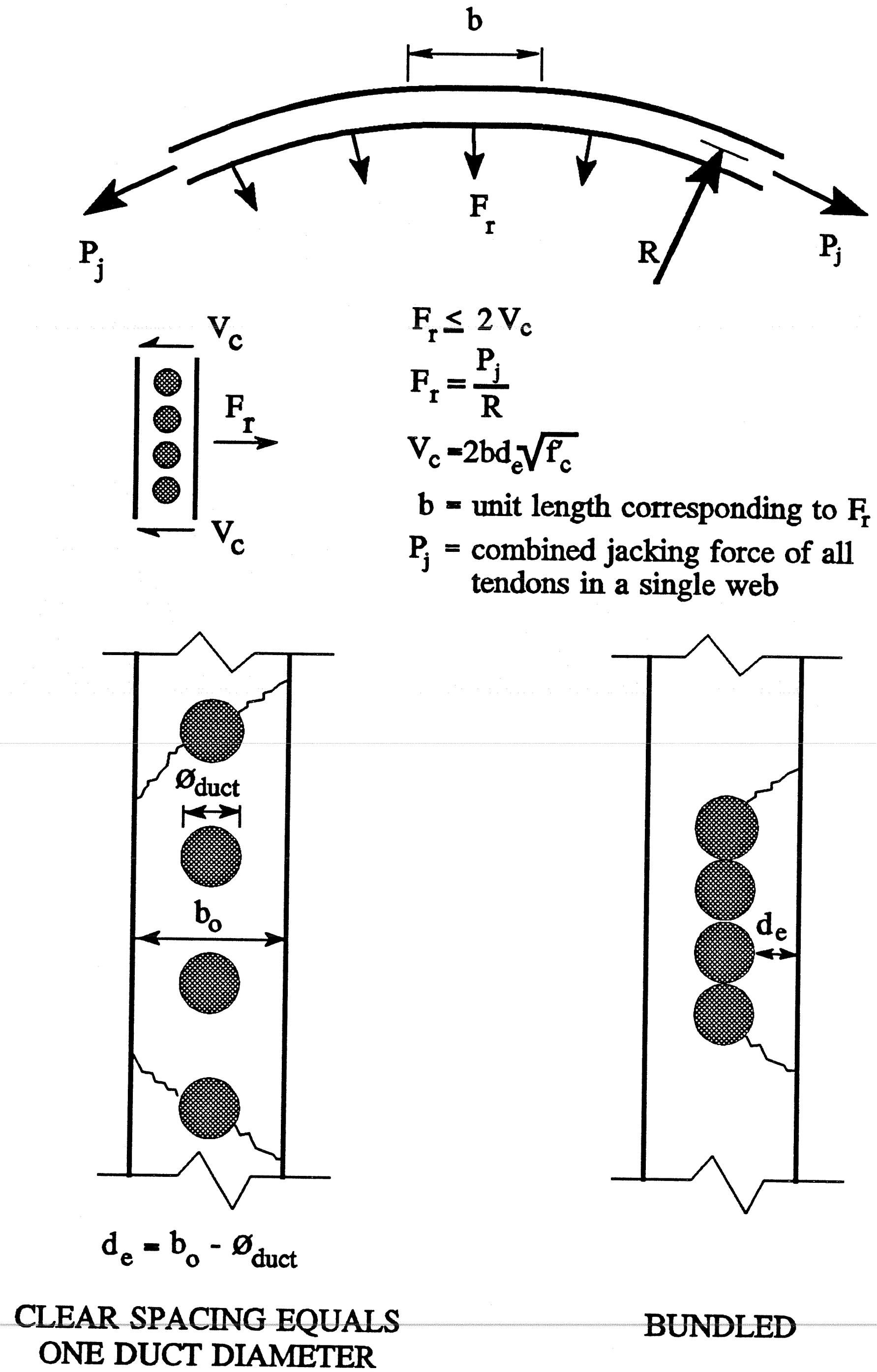

Figure 5.31 Design Criteria For Radial Shear

Chapter 6
CONCLUSIONS AND RECOMMENDATIONS

6.1 Summary of the Test Program

Curved post-tensioned box girders are used in curved ramps and curved bridges. Cracking problems in curved box girders have been known to exist during post-tensioning but until recently were often ignored. However, this changed with the disastrous failures of the Kapioloni ramp in Hawaii and the Las Lomas bridge in California, both of which failed during the post-tensioning process. In both of the failures the tendons broke out of the inside face of the web. It is believed that these failures occurred due to the combination of sharp radius of curvature, close duct spacing, high post-tensioning forces, insufficient duct cover on the inside face of the web and insufficient stirrups in the web. There has apparently been no experimental investigation reported which studied the resistance of curved box girders to breakout forces during post-tensioning. Based on theoretical studies, CALTRANS has suggested web detailing requirements for post-tensioned box girders with a sharp radius of curvature. These requirements vary with change in radial force(F_r), web height and the reinforcing steel. A test program was developed at the Phil M. Ferguson Structural Engineering Laboratory to study the effect of duct spacing on the resistance to breakout forces in horizontally curved box girders during post-tensioning.

Experimental investigation was initiated by design and construction of a one-third scale model of a typical single cell box girder. The section dimensions were one-third in scale of the failed Las Lomas bridge. 6mm grade 75, Swedish bars were used for all reinforcing. The duct arrangements in the two webs of the box girder were different. One of the webs(BC) was detailed to have bundled ducts in the curved region. The other web(DC) was detailed to have ducts spaced at a clear spacing of one duct diameter in the curved region. A pilot test setup was designed and assembled so as to apply uniform jacking load to the tendons at the web ends. Each strand was seated and stressed separately to a predetermined load.

Instrumentation devices were installed to measure and record the strains in the stirrups, delamination of the web, web deflection and the applied load.

Each web was loaded separately in increments until it failed. Each web failed in a different manner. Web DC exhibited a brittle and explosive failure. It failed without any visual or audible warning. Web BC on the other hand failed with some visual and audible warning. In the case of the web BC, large cracks were observed one foot above and below the center line of the duct arrangement.

6.2 Conclusions

The following limited conclusions can be drawn based on the two tests conducted:

1) A web with ducts positioned at one duct clear spacing has more than twice the ultimate radial load capacity(as measured) than a web with bundled tendons.

2) Failure in both of the webs was principally due to failure of the web concrete in shear-diagonal tension.

3) In the case of the web with bundled tendons, the concrete over the duct on the inside face of the web acts somewhat as a local beam. This local beam action dominates the behavior of the web with bundled tendons.

4) In the case of the web with spaced tendons, the overall section seemed to be more of an influence.

5) Checks of the flexural capacity of the web indicates that substantial load must be transferred to the ends by arch action.

6.3 Design Recommendations

1) If the ducts are bundled in the curved region then the ultimate flexural capacity of the local beam should be checked. The local beam can be assumed to span from the top of the top-most duct to the bottom of the bottom-most duct. The thickness of the beam can be assumed as the dimension of the cover over the duct on the inside face of the web. This local beam can be assumed to be fixed at its ends which can be taken at the ends of the duct region.

2) Webs should be checked for radial shear. In the absence of the transverse tie bars radial shear resistance shall be provided only by concrete

shear strength. Concrete shear resistance shall not be assumed as greater than $2\sqrt{f_c'}$ unless the ratio of shear and moment is checked(V_u/M). This recommendation should be conservative and should be followed until further tests are conducted. Detailed design recommendations for radial shear are described in Section 5.2.

If the web with bundled tendons fails to meet the shear design criteria, then the duct spacing should be increased to one duct clear spacing. If the web with ducts spaced at one duct clear spacing fails to meet the radial shear criteria then the web thickness should be increased or the web redesigned.

6.4 Future Research

Further experimental investigation is required to fully understand the effect of duct spacing and other parameters on a curved box girder during post-tensioning. Webs with duct spacing in between the extremes of bundled ducts and ducts spaced at one duct clear spacing should be tested. Effect of other parameters such as duct cover on the inside face of the web and varied reinforcement patterns should be investigated experimentally. It would be interesting to position the ducts at an offset(not in the center of the web) and vary the duct spacing. Tests should be conducted to test the effectiveness of the detailing reinforcement requirement suggested by CALTRANS. Tests should also be conducted to study the effect of varying the stirrup spacing on the ultimate capacity of the web. A finite element analysis model of the web would be an interesting analytical tool. With further research the design recommendations can be further validated and modified if required.

REFERENCES

1. Podolony W. and Muller J., Construction and Design of Prestressed Concrete Segmental Bridges, John Wiley and Sons, 1982.
2. Figg and Muller Inc., Prestressed Concrete Segmental Bridge Construction Manual, Bridge Engineers Seminar, Asheville, North Carolina, 1981.
3. 'Ramp Cracking Explained', ENR, September 22,1983, page 18.
4. Podolony W.,'The Cause of Cracking in Post-Tensioned Concrete Box Girder Bridges and Retrofit Procedures', Journal of Prestressed Concrete Institute, vol. 30, no. 2, March/April 1985.
5. 'Las Lomas Bridge - Causes of Structural Failure', Report to Department of Army, San Francisco District Corp. of Engineers, T. Y. Lin International, August 1979(unpublished).
6. Taylor A.W.,'Behavior of Thin Walled Hollow Concrete Bridge Piers & Pylons', Phd Dissertation, The University of Texas at Austin, December 1990.
7. ZumBrunnen L.G.,'Behavior of Statically Loaded Prestressed Concrete Girders with 0.5 inch Diameter', Masters Thesis, The University of Texas at Austin, May 1991.
8. Moe J., Shearing Strength of Reinforced Concrete Slabs and Footings under Concentrated Loads, Portland Cement Association Research & Development Laboratories, Skokie, Illinois, Development Department Bulletin D47, April 1961
9. Shear and Diagonal Tension, Report of ACI-ASCE Committee 326, 1962
10. Breen J. E. and Pauw A., An Investigation of the Flexural and Shearing Capacity of Reinforced Concrete Beams, The University of Missouri Bulletin, vol. 61, no. 33, Engineering Series No. 49, University of Missouri, Department of Civil Engineering, Columbia, Missouri, July 1960.

11. Ferguson, Breen, Jirsa, Reinforced Concrete Fundamentals, fifth edition, John Wiley & Sons, Inc., New York, 1988.
12. Lin T.Y. and Burns N.H., Design of Prestressed Concrete Structures, third edition, John Wiley & Sons, Inc., New York, 1981.
13. Standard Specifications for Highway Bridges, fourteenth edition, American Association of State Highway and Transportation Officials(AASHTO), 1989.
14. Building Code Requirements for Reinforced Concrete(ACI 318-89) & Commentary - ACI 318R - 89, American Concrete Institute, Detroit, 1989.

VITA

Deepak Ahuja was born in Kanpur, India on August 4, 1966, the eldest of the two children of Kavita Ahuja and Srichandlal Kishanchand Ahuja. He graduated from the Methodist High School with the ICSE certificate in April, 1981 and with the ISC certificate in April, 1983. He entered the Birla Institute of Technology(BIT), Ranchi, India in September 1983. He graduated with distinction in June, 1987 and was awarded the degree of Bachelor of Engineering in Mechanical Engineering. From 1987 to 1989 he pursued his second degree in Civil Engineering at the Birla Institute of Technology. He graduated with distinction in May, 1989 and was awarded the degree of Bachelor of Engineering in Civil Engineering. In January, 1990 he entered the Graduate School of the University of Texas at Austin.

Permanent Address: 122/731, Shastri Nagar,
Nandpuri,
Kanpur - 208005
India

This report was typed by Deepak Ahuja